GROUND MOTION PREDICTION EQUATIONS (GMPES) FOR SUBDUCTION-ZONE EARTHQUAKES IN JAVA ISLAND, INDONESIA

BY

ABDUL LATIF ASHADI

A Thesis Presented to the
DEANSHIP OF GRADUATE STUDIES

KING FAHD UNIVERSITY OF PETROLEUM & MINERALS

DHAHRAN, SAUDI ARABIA

In Partial Fulfillment of the
Requirements for the Degree of

MASTER OF SCIENCE

In

GEOPHYSICS

MARCH 2015

KING FAHD UNIVERSITY OF PETROLEUM & MINERALS

DHAHRAN- 31261, SAUDI ARABIA

DEANSHIP OF GRADUATE STUDIES

This thesis, written by **ABDUL LATIF ASHADI** under the direction his thesis advisor and approved by his thesis committee, has been presented and accepted by the Dean of Graduate Studies, in partial fulfillment of the requirements for the degree of **MASTER OF SCIENCE IN GEOPHYSICS.**

Dr. SanLinn Ismail Kaka
(Advisor)

Dr. Abdulaziz Al-Shaibani
Department Chairman

Dr. Abdullatif A. Al-Shuhail
(Member)

Dr. Salam A. Zummo
Dean of Graduate Studies

Dr. Michael Kaminski
(Member)

14/4/15
Date

Dedicated to my beloved country, Indonesia

ACKNOWLEDGMENTS

All praise and thanks be to Allah, all gratitude belongs to Allah the Lord of the universe, Who gives people knowledge that they know not. I thank Allah for bestowing on me His mercy. Then I would like to express my grateful to all people who helped and encouraged me for finishing my thesis.

I gratefully acknowledge King Fahd University of Petroleum and Minerals for giving me opportunity to pursue my master degree in geophysics program.

I would like to express my sincere appreciate to the Earth Sciences Department and the Chairman Dr. Abdulaziz Al-Shaibani for his help and support.

I am deeply indebted to my supervisor Dr. Sanlinn Isma'il Kaka for his insightful advice, suggestions and motivation. I thank him, as he is indeed not only advisor but father to reckon with.

My sincere thanks are due to my thesis committee members: Dr. Abdullatif A. Al-Shuhail and Dr. Michael Kaminski, for their constructive criticism and suggestions that are very helpful.

I also feel grateful to all my colleagues and friends at KFUPM, especially the Indonesian student community for their support, encouragement and suggestions.

TABLE OF CONTENTS

LIST OF TABLES

LIST OF FIGURES

LIST OF ABBREVIATIONS

ASCE	The American Society of Civil Engineers
AB-2003	Atkinson and Boore (2003)
BMKG	The Indonesian-Meteorological Climatological and Geophysical Agency
F_1(**M**)	Magnitude scaling
F_2(**M**,R_{rup},H)	The distance and depth scaling
F_3(Z_T)	The source type (interface or in-slab) fauction
fn(**M**)	The function relevant to the magnitude
GCMT	The Global Centroid Moment Tensor
GMPEs	Ground Motion Prediction Equations
H	The focal depth (km)
h_{hypo}	The hypocentral depth (km)
IBC	International Building Code
ISC	The International Seismological Centre
M	Moment magnitude

m_b	Body wave magnitude
M_L	Local magnitude
M_S	Surface wave magnitude
MWO	World Meteorological Organization
NEIC	The National Earthquake Information Centre
NEHRP	National Earthquake Hazard Reduction Program
n	The amount of data recordings
PSHA	Probabilistic seismic hazard analysis
p	The number of regression coefficients
PGA	Peak ground acceleration
R_{epi}	The epicenteral distance
R_{jb}	The closest horizontal distance to vertical projection of the fault rupture plane
R_{hypo}	The hypocentral distance
R_{rup}	The closest distance to rupture plane (km)
R_{seis}	The closest distance to the seismogenic part of the fault rupture plane
S	The magnitude dependence of the geometric spreading coefficient

SA	Spectral acceleration
SMA	Strong-motion accelerograph
USGS	The United States Geological Survey
V_S^{30}	The shear-wave velocity of the top 30 m of the subsurface
Youngs-97	Youngs et al. (1997)
Y	Spectral acceleration (g)
Z_T	Source type, 0 for interface and 1 for in-slab earthquakes
Δ	A near-source saturation term

ABSTRACT

Full Name : Abdul Latif Ashadi

Thesis Title : Ground Motion Prediction Equations (GMPEs) for Subduction-Zone Earthquakes in Java Island, Indonesia

Major Field : Geophysics

Date of Degree : February, 2015

In this research, I present predictive relations for peak ground acceleration (PGA) and response spectral acceleration (PSA) at frequencies of 1, 2 and 5 Hz for subduction-zone earthquakes in Java Island. The dataset includes 1,574 strong-motion recordings from 118 subduction-zone earthquakes of moment magnitude (**M**) 4.4 to 7.0 that occurred between 2008 and 2013. The predictive relations are developed for both interface and in-slab events on NEHRP (National Earthquake Hazards Reduction Program) class B. These relations are important because Java Island is a seismically active and densely populated region in Indonesia and there are no region-specific ground-motion relations for the island. Available relations (Youngs et al., 1997 and Atkinson and Boore 2003) were found to be unreliable in predicting previously recorded moderate subduction events in Java Island, in particular for moderate events (**M** $\leq$ 6.0). Thus, I undertook this study to develop a ground-motion relations specific to Java Island. My resultant predictions are generally lower than those predicted by Youngs *et al*. (1997) and significantly higher for moderate events than those of Atkinson and Boore (2003). Predicting ground shaking is a key step in anticipating earthquake effects in the region. The ground-motion predictive

relations developed in this study can be used for probabilistic seismic hazard studies in Java Island to estimate the hazard.

ملخص الرسالة

الاســـــم الكـامـــل : عبد اللطيف أشهدي

عنوان الرســـالـــة : ذروة التسارع الأرضي التنبؤ (GMPEs) عن الزلازل الاندساسية منطقة في جزيرة جاوا الإندونيسية

التـــخـــصـــــص : جيوفيزياء

تاريخ الدرجة العلمية : فبراير2015

في هذه الاطروحة تمت دراسة العلاقة بين ذروة التسارع الأرضي و استجابة تسارع الطيفي اثناء حدوث الزلزال لثلاثة ترددات موجية مختلفة وهي1، 2 و 5، وذلك في نطاقات الانضوأء الزلزالية لجزيرة جاوا الاندونيسية. البيانات المستخدمة تضمنت 1,574 تسجيل زلزالي ذو شدة عالية اخذت من 118 هزة ارضية في نطاقات انضوأء زلزالية ذات مقياس درجة العزم بين 4.4 الي 7.0 في فترة ما بين عامي 2008 و2013. الغرض الاساسي من استحداث هذا النموذج كان لتنبأ بالهزات الاراضيه الناتجة من النطاقات الضحلة والعميق ، اتبع في استحداث هذا النموذج مواصفات برنامج القومي لحد من مخاطر الزلازل (NEHRP) تصنيف (ب). تكتسب هذه نوعية من الدراسة اهمية بالغة نسبة لكثافة سكانية عالية ، نتيجة لنشاط الزلزالي مستمر، وعدم توفر نماذج لتنبأ بالزلازل في منطقة جاوا. وبالاضافة الي النماذج المتفورة حاليا (Youngs et al., 1997 and Atkinson – Boore, 2003) تتميز بعدم دقة في استنتاج الهزات الارضية السابقة في

منطقة الدراسة خصوصا لاحداث الانضواء ذات درجة عزم متوسط (**M** ≤ 6.0). وعليه، هذه الاطروحة اهتمت بتطوير نموذج يستطيع تقدير حركية الارض لجزيرة جاوا. اظهرت هذه الاطروحة نتائج تعتبر اقلة دقة مقارنة مع نموذج Younges et al., (1997) ونسبيا افضل من نموذ Atkinson and Boore (2003) في تنبأ بالاحداث الانضواء ذات درجة عزم متوسط. التنبأ بالهزات الاراضية يعتبر حجر زاوية في في استنتاج التاثير الناتج عن الهزات الارضية . نموذج حركية الارضية المستحدث في هذه الدراسة يمكن استخدامة في دراسة المخاطر النامجة من هزات الارضية في جزيرة جاوا.

CHAPTER 1

INTRODUCTION

1.1 Overview

Earthquakes are the result of a sudden energy released in the Earth's crust which produces seismic waves. These waves propagate from the focus of the earthquake to all directions in the earth. When seismic waves reach the earth's surface, the vibrations can damage or not, it depends on the source energy and the distance, and quality of construction and the site where building stands. The wave velocity will be recorded by a seismograph, while the wave acceleration will be recorded by an accelerograph (ground acceleration recording or strong-motion accelerograph [SMA]). Advent of an earthquake cannot be denied or avoided, but sought for disaster risk can be minimized. The most important way is to know the earthquake behavior of structures, where an understanding of ground motion is most essential (Housner, 1970).

The importance in understanding earthquake behavior of structure is a must. Since undesirable effects of this phenomenon result in huge damage both in environment and living things. For example, an earthquake potentially triggers tsunami, landslides, fault rupture, fire, and the greatest effects come from collapse of infrastructure. From this stand

point, to design earthquake-resistant structures by understanding strong ground motions can be the effective solution for earthquake disaster mitigation.

The Indonesian region is one of the most seismically active zones in this earth. Because the tectonics of Indonesia are very complex, as it is a meeting point of several tectonic plates (Bird, 2003). Indonesia is located between two continental plates: the Eurasian Plate and Indian-Australian Plate; and between two oceanic plates: the Philippine Sea Plate and Pacific Plate (Hall, 2002). This condition can be figured in Figure 1. Therefore, this study is extremely important for Indonesia, especially for the Java Island region. Java Island was selected for this research because most of the populated metropolitan areas, infrastructure, and main government facilities in Indonesia are concentrated in this island.

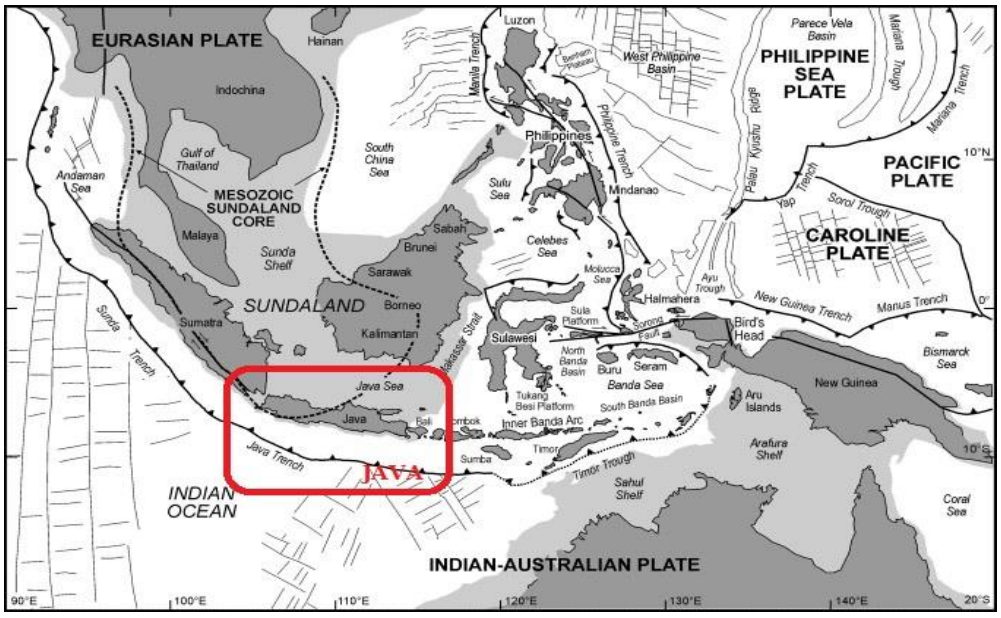

Figure 1 Principal geographical features and plate tectonics of South East Asia (Hall, 2002).

1.2 Problem Statement

As a country prone to earthquakes and considering the high damage, Indonesia should encourage all study related to earthquake engineering. The most important is to know is the earthquake behavior of structures, where an understanding of ground motion is most essential. To date, there are no published empirical GMPEs specifically developed for Indonesia region. Although the Indonesia Government has revised the maps of Indonesian seismic hazards in 2010, then used them in the Indonesian Earthquake Resistant Building Code in 2012 (SNI-1726-2012), but the results did not used specific GMPEs for the Indonesia region. Java Island, the most populated metropolitan area in Indonesia, is one of the high seismically active regions in Indonesia. The seismicity is mainly caused by subduction zone earthquakes. Therefore, a study of GMPEs specifically developed for subduction zone earthquakes is necessary.

1.3 Thesis Objectives

The aim of this work is to perform regression analyses using the least square method to develop GMPEs for peak ground acceleration (PGA) and 5% damped response spectral acceleration (SA) at frequencies of 1, 2, and 5 Hz on rock (NEHRP B). These GMPEs are specifically developed for subduction zone earthquakes in Java Island. The regression is based on two horizontal-components of digital accelerograph data from 118 subduction zone earthquakes of moment magnitude (**M**) greater than or equal to 4.4 that

occurred between 2008 and 2013 in the south of Java Island. Java Island was selected for this research because most of the populated metropolitan areas, infrastructure, and main government facilities are concentrated on this island.

1.4 Thesis Outline

The thesis consists of five chapters. Chapter one provides a general background and description for the thesis, and also the literature review. Chapter two gives succinct introduction to the seismicity of Java Island and strong motion network in Indonesia. Chapter three illustrates the ground motion prediction equations (GMPEs) used in this thesis. This chapter describes the methodology and the model parameters such as, ground motion parameters, earthquake magnitude scales, source to site distance and local site condition.

Chapter four is the key part of the thesis. This chapter discusses the regression analysis process, such as, illustrating how to select and process the dataset, as well as shows the results and their comparison with previous studies. The last chapter concludes the work done in this thesis and proposes some recommendation for future research.

1.5 Literature Review

Many studies on GMPEs have already been carried out in various places. Douglas (2011) compiled all empirical ground-motion prediction equations (GMPEs) published between 1964 and 2010. He summarized the characteristics of 289 empirical GMPEs used to determine the PGA prediction and 188 empirical models used to determine the prediction of elastic response spectral ordinates (Douglas, 2011). However, only a few GMPEs are given for the category of subduction zone earthquakes.

Youngs et al. (1997) developed ground motion attenuation relationships for peak ground acceleration (PGA) and the response of spectral acceleration for subduction zone earthquakes. These authors used 350 horizontal-component response spectra of earthquake data compiled from Cascadia, Japan, Alaska, Chile, Mexico, Peru, and the Solomon Islands. The data are from interface and in-slab earthquakes of moment magnitude 5 and greater and for the closest distance to the rupture plane (R_{rup}) of 10 to 500 km.

The resultant relationships of Youngs et al. (1997) are given by:

$$\mathrm{Ln}(y) = C_1 + F_1(\mathbf{M}) + F_2(\mathbf{M},R_{rup},H) + F_3(Z_T) \tag{1.1}$$

where $F_1(\mathbf{M})$ is magnitude scaling given by the function:

$$F_1(\mathbf{M}) = C_2 + C_3\,(10 - \mathbf{M})^3, \tag{1.2}$$

$F_2(\mathbf{M},R_{rup},H)$ is distance and depth scaling given by the function:

$$F_2(\mathbf{M},R_{rup},H) = C_4 \ln(R_{rup}) + C_5 \exp(C_6\mathbf{M}) + C_7H, \quad (1.3)$$

$F_3(Z_T)$ is the source type (interface or in-slab) given by the function:

$$F_3(Z_T) = C_8Z_T, \quad (1.4)$$

In these equations, y is the spectral acceleration (g); **M** is the moment magnitude; R_{rup} is the closest distance to the rupture plane (km); H is the focal depth (km); and Z_T is the source type, 0 for interface and 1 for in-slab earthquakes.

Atkinson and Boore (2003) developed empirical GMPEs for subduction zone earthquakes using a maximum likelihood regression method. They compiled a response spectra database from 1,148 horizontal-component records of ground-motion recordings with moment magnitudes 5-8.3 occurring in subduction zones around the world. The number of earthquakes used is 77 with a rupture distance range of 10 to 500 km.

The ground motion model of Atkinson and Boore (2003) is:

$$\text{Log}_{10}(y) = F(\mathbf{M}) + C_3H + C_4R - g \log_{10}(R) + C_7 \text{ sl } S_C + C_8 \text{ sl } S_D + C_9 \text{ sl } S_E \quad (1.5)$$

Where $F(\mathbf{M})$ is a function relevant to the magnitude given by the equation:

$$F(\mathbf{M}) = C_1 + C_2\mathbf{M}, \quad (1.6)$$

g is the magnitude dependence of the geometric spreading given by the equation:

$$g = 10^{C_5 + C_6\mathbf{M}}, \quad (1.7)$$

$$R = \sqrt{{R_{rup}}^2 + \Delta^2}, \quad (1.8)$$

$$\Delta = 0.00724 \text{ x } 10^{0.507\mathbf{M}}, \quad (1.9)$$

where y is in cm/s^2 and Δ is a near-source saturation term.

The latest subduction GMPEs are attenuation functions developed by Lin and Lee (2008) for northeastern Taiwan. The database used in this study is 54 earthquakes: 17 interface earthquakes, and 37 in-slab earthquakes, including 4,823 sets of three-component records. The moment magnitude range is between 4.1 and 8.1 with a hypocentral distance range of 20 to 600 km. The resultant equation regressed by the least square method (LSM) is:

$$\mathrm{Ln}(y) = C_1 + C_2\mathbf{M} + C_3 \ln(R_{\mathrm{hypo}} + C_4 \exp[C_5\mathbf{M}]) + C_6 H + C_7 Z_{\mathrm{T}} \qquad (1.10)$$

where y is the ground acceleration (g) and R_{hypo} is the hypocentral distance (km).

CHAPTER 2

SEISMICITY OF JAVA ISLAND

2.1 Overview

Java Island is located close to a subduction zone (Java Trench) which makes it one of the most seismically active regions in Indonesia. The Indian-Australian Plate is subducting beneath the Eurasian Plate along the Java Trench, located in the south of Java Island. Historically, there have been several large earthquakes that struck the island of Java. According to historical data, in the south of Java Island, there were at least three large earthquakes: on September 11, 1921, with a compute magnitude (M_c) of 7.92 as an intraplate event; on September 27, 1937, with a compute magnitude of 7.2 that is regarded as an in-slab event; and on July 23, 1943, with a moment magnitude of 8.1 (Okal, 2012). Moreover, in the instrumental seismogram period, more earthquakes were flawed.

On June 3, 1994, a tsunami earthquake with **M** of 7.6 occurred along the southeast coast of Java Island about 240 km from the nearest coast. The tremor was felt on East Java and on Bali Island and killed about 233 persons (Tsuji *et al.*, 1995; Abercrombie *et al.*, 2001). On May 27, 2006, a **M** 6.3 earthquake struck south of Central Java, about

20 km from Yogyakarta, causing 5,176 deaths and injuring over 40,000 people. The total amount is estimated at US $3.1 billion in damage (CGI, 2006), making it one of the most costly natural disasters in the last ten years (Hutapea *et al.*, 2006; Tsuji *et al.*, 2009). Two month later, exactly on July 17, 2006, a **M** 7.7 struck the south coast of West Java, about 355 km south of the capital Jakarta or about 200 km south of western Java Island. The earthquake caused a tsunami with wave of up to 5 meters and killed at least 600 people. More than 230 people are still missing and feared dead. At least 75,000 people were displaced and 1,513 buildings damaged in West Java and in Central Java Province (Kato *et al.*, 2007; Mori *et al.*, 2007). After that, on September 2, 2009, at least 80 people were killed and 1,115 people were injured by an earthquake of **M** 7.3 that struck the south coast of West Java. The earthquake did not produce a tsunami, but it caused several damage to more than 67,000 houses (Boen *et al.*, 2009). During 1960 to 2012, there were 1,172 earthquakes with a moment magnitude more than 5 occurring in the Java Island region. The seismicity of Java Island can be seen in Figure 2.

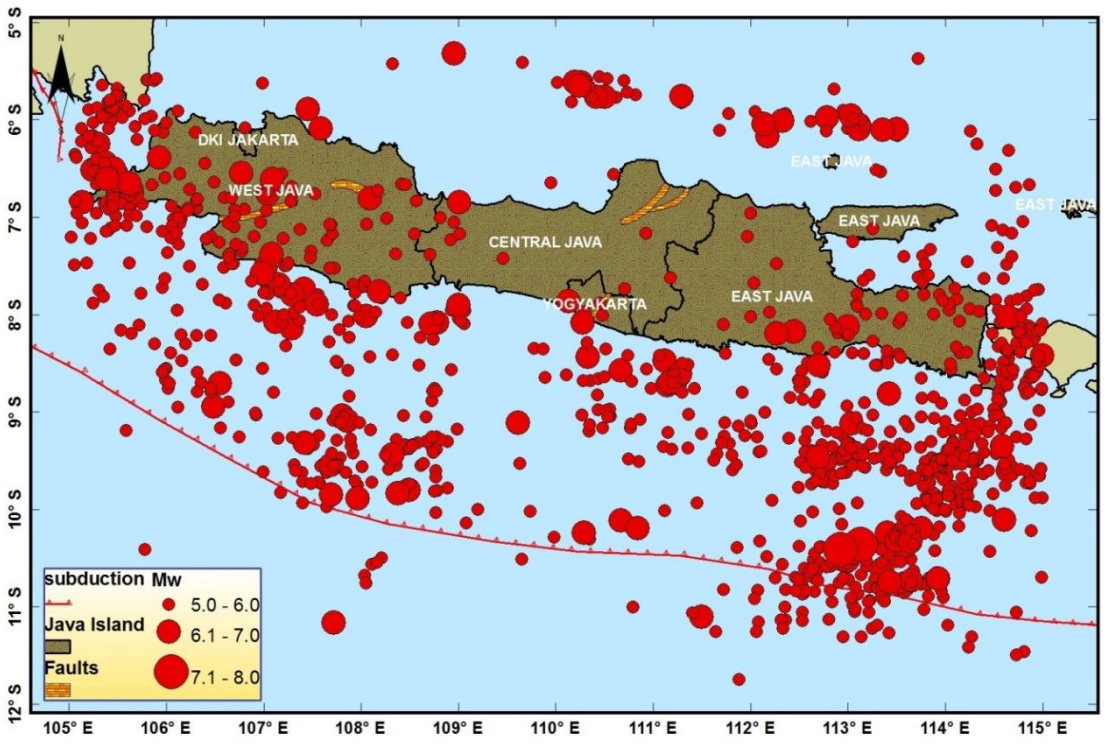

Figure 2 Seismicity of Java Island for the period of 1960 to 2012 (developed by the author).

2.2 Seismotectonics of Java Island

With a population of 141 million (in 2012), Java island is one of the most densely populated regions in Indonesia. Java is the residence of 60 percent of the Indonesian population. The Java area, including nearby islands, is 49,976 square miles (129,438 square km). In this island, two plates with different of movement types formed several active faults, several active mountains, and subduction zones. The subduction zone is known as the "Java Trench" or "Sunda Arc". The Indian-Australian Plate is subducting beneath the Eurasian Plate along the Java Trench located in the south of Java Island. The average distance between the Java Trench and the south coast of Java Island is

approximately 200 km. Therefore, the most events occurred in Java Island are in the far distance.

Along the south coast of Java Island, the Indian-Australian Plate is moving toward the Eurasian Plate at various velocity: 6.3 cm per year at N14° south of the Sunda Strait (west of Java Island); 6.7 cm per year at N14° south of Central Java; and 7.0 cm per year at N13° south of the Bali Sea (east of Java Island) (Simons *et al.*, 2007; Pacey *et al.*, 2013) (see Figure 1). Figure 2 shows the cross section of the subduction zone beneath Java Island.

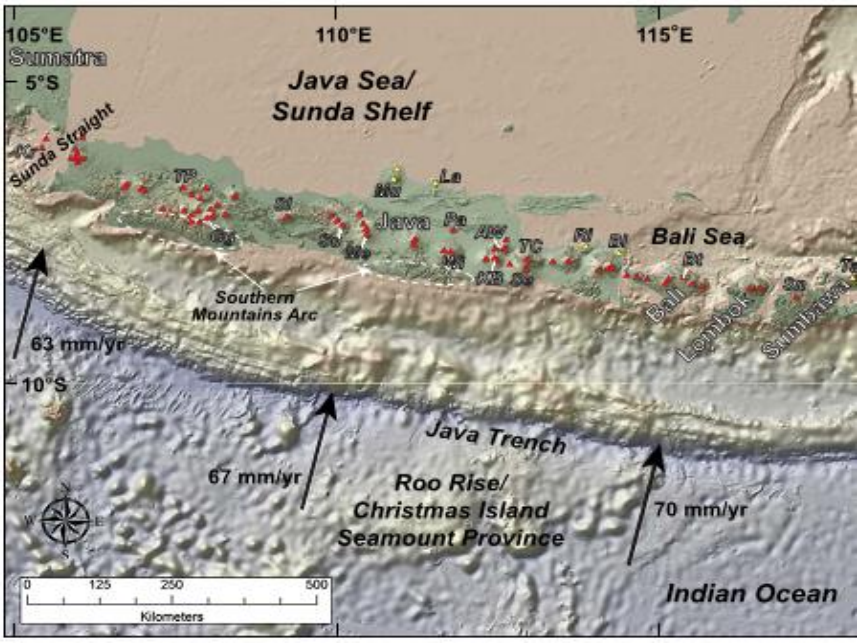

Figure 3 Relief of direction and motion in the Java Trench located south of Java Island (Pacey *et al.*, 2013).

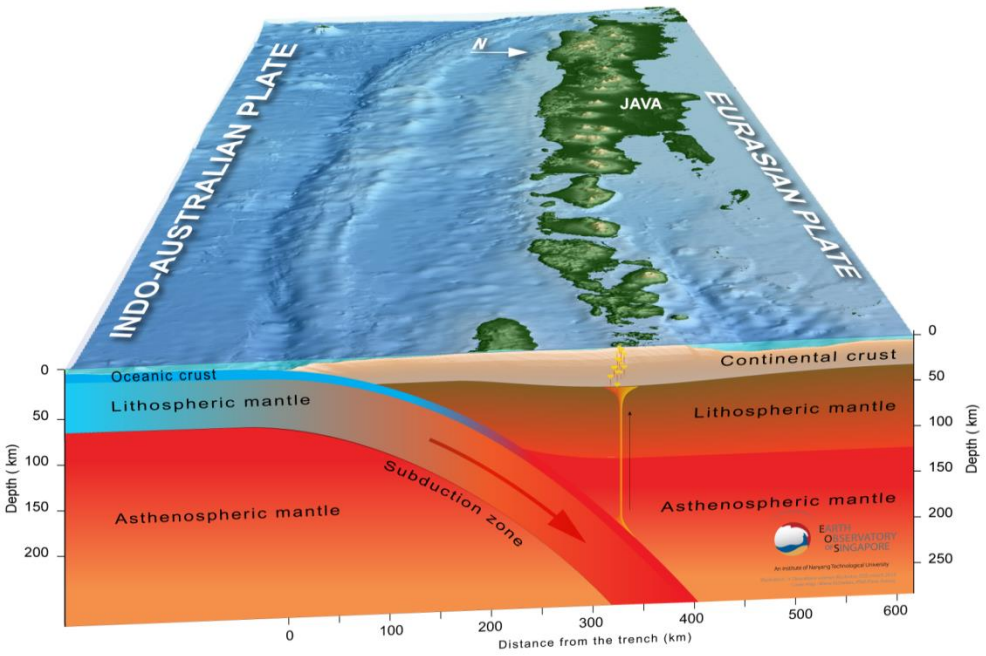

Figure 4 Cross-section of the subduction zone beneath Java Island (http://www.earthobservatory.sg).

2.3 Strong Motion Network in Java Island

The accelerograph is an instrument that records the ground acceleration during an earthquake. It can be used to monitor structures for earthquake response and to improve the building design, or to help locate important structures in safer areas. Commonly it has three components: two horizontal components and a vertical component. Indonesia as a country highly prone to earthquakes ought to have a good accelerograph network system. In fact, Indonesia began to build a good accelerograph network in 2005 after the catastrophic 2004 Indian Ocean tsunami that killed over 230,000 people in fourteen countries. The network that can be accessed well was initiated in 2008.

Until 2010, the Meteorological Climatological and Geophysical Agency (BMKG) had 210 accelerograph stations, with 69 of them located in Java. The location of accelerographs can be seen in Figure 5. The BMKG is the official institution for Meteorological Climatological and Geophysical in Indonesia since 1947, and has affiliated with the World Meteorological Organization (MWO) since 1950. The function of the BMKG includes the implementation, monitoring, and control of observations, and processing of data and information in the area of meteorology, climatology, and geophysics in Indonesia.

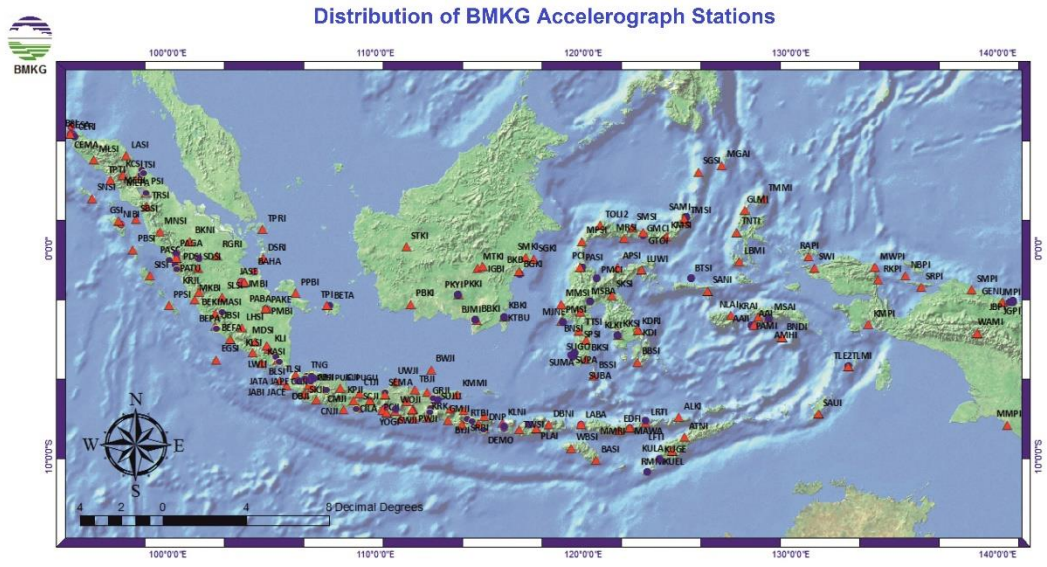

Figure 5 Distribution of BMKG accelerograph stations updated in 2013 with 69 located in Java. (http://www.bmkg.go.id/).

The Indonesian accelerograph consists of two types: the Geodivice BBSA-2 and the Metrozet TSA-100S. Both can affect the coefficient factor (CF) that is used to compute the actual peak ground acceleration (PGA). Network configurations pay

attention not only to the level of density, but also to the source of the earthquake and the rate of population growth and development of the city (Suhardjono, 2010).

CHAPTER 3

GROUND MOTION PREDICTION EQUATIONS

3.1 Overview

The ground motion prediction equations (GMPEs, also known as attenuation equations) are one of the most important parameters in probabilistic seismic hazard analysis (PSHA). GMPEs are used to estimate ground motion parameters such as PGV, PGA, or PSA for an earthquake, given the magnitude, distance, and site conditions. These equations are developed empirically by a regression of recorded strong-motion amplitude data versus magnitude, distance, and possibly other predictive variables (Bozorgnia and Bartero, 2004). An applicable attenuation equation not only helps the seismologists to understand several characteristics of ground-motion attenuation, but also predict the ground-motion values for a specific site. Finally, they can be considered when appropriately designing earthquake-resistant structures.

To determine the GMPEs, there are two different methods: theoretically, using models for generating synthetic ground motions that account for the source, site, and path effects, or empirically, using previously recorded ground motions. The most commonly used ground motion parameters are vertical and horizontal components of PGV, PGA,

and 5% damped PSA for a given site condition. There are three categories of regional GMPEs normally used in seismic hazard assessments: shallow crustal earthquakes in active tectonic regions, subduction zone earthquakes, and shallow crustal earthquake in stable continental regions (Abrahamson and Shedlock, 1997).

Many studies on GMPEs have already been carried out in various places. The relevant studies in this category are Youngs et al. (1997), Atkinson and Boore (2003), Zhao et al. (2006), and Lin and Lee (2008). However, there are no GMPEs specifically developed for Indonesia region due to unavailable data of ground motion recordings (accelerograph). Recently, Megawati and Pan (2009) developed GMPEs for the Sumatran-Indonesia megathrust earthquakes, based on synthetic seismograms using a finite-fault kinematic model.

3.2 Methodology

To develop specific GMPEs for subduction zone earthquakes, I processed with the following steps:

1. Collecting database from two horizontal-components of BMKG's accelerographic network recording from subduction zone earthquakes in south Java Island from 2008 to 2013. The processed ground motion parameters are PGA and PSA at frequencies of 1, 2, and 5 Hz.

2. Understanding local site conditions of each accelerograph station location using the 30-m shear-wave velocity (V_S^{30}). The V_S^{30} data are compiled from the BMKG and the Global V_S^{30} Map Server from the USGS.

3. Applying the amplification factor from the American Society of Civil Engineers (ASCE) into each accelerograph station recording that produce the PSA on rock (NEHRP B).

4. Converting magnitude scales into moment magnitude estimated by HVRD (GCMT solution, **M**). The conversion was performed using the equation proposed by Abe (1981), Scordilis (2006), and Irsyam et al. (2010).

5. Determining the closest distance to the fault rupture plane (R_{rup}). This is done using the equation proposed by Wells and Coppersmith (1994) that predicts fault length and area as a function of moment magnitude.

6. Classifying the compiled database into two types: interface and in-slab subduction events.

7. Fitting the database by the method of least squares for different forms of GMPEs. This step includes the determination of the geometric spreading coefficient (*S*) by preliminary regression.

8. Comparing the predicted equations to the observed database corresponding to predictions of previous equations developed for worldwide subduction zone earthqukaes, e.g. Young et al. (1997) and Atkinson and Boore (2003).

3.3 Ground Motion Parameters

Like some previous GMPEs for subduction zone earthquakes, e.g., Young et al. (1997); Atkinson and Boore (2003); Lin and Lee (2008), the ground motion parameters used are PGA and 5% damped PSA in several periods from both interface and in-slab subduction earthquakes.The strong- motion parameters regressed in this study are PGA and PSA at frequencies of 1, 2, and 5 Hz. They represent the maximum absolute amplitude of the ground motion measured from the recorded accelerograpic network.

3.4 Earthquake Magnitude

There are many different scales to define earthquake magnitude, e.g. local magnitude (M_L), body wave magnitude (m_b), and surface wave magnitude (M_S), but all of the subduction ground motion relations discussed in this study use moment magnitude (**M**). The moment magnitude can be designated as M_W or **M**. **M** is derived from the seismic moment which is uniformly valid to all sizes of earthquake magnitudes and measures the energy radiated by an earthquake (Bozorgnia and Bertero, 2004). Although it represents the size of an earthquake only at a period much longer than the source process time, it can be determined very accurately from seismograms (Kanamori, 1983).

During the period from March 2008 to February 2013, 118 earthquakes were recorded in south Java Island and they were classified as subduction zone earthquakes. Due to unavailable earthquake source parameter data (epicenter, focal depth, magnitude,

and focal mechanism) from the BMKG, I compiled them from the Global Centroid Moment Tensor (GCMT, formerly known as the Harvard CMT catalog). If the GCMT data were not available, then epicenter location and magnitude from the International Seismological Center (ISC) or the National Earthquake Information Center (NEIC) catalogs were used. The compiled source parameter data consists of the following numbers; 41 of the **M** data are from the GCMT; 17 of the m_B data are from the ISC; 22 of the m_b are from the ISC; 22 of the M_L are from the ISC; 23 of the m_B data are from the NEIC; and 12 of the m_b are from the NEIC. Then I converted the magnitudes from the ISC and the NEIC, using the conversion equations proposed by Abe (1981), Scordilis (2006), and Irsyam et al. (2010) to **M** released by the Harvard CMT catalog, thus keeping the magnitudes on the same scale. The list of earthquakes used in this study is summarized in Table 1, while Figure 6 shows the locations of accelerograph stations and analyzed earthquakes.

Table 1 List of earthquakes used to develop GMPEs.

NO	Earthquake	Date	Lat.	Lon.	H (km)	M
Interface Earthquakes						
1	Blitar	31-03-2008	-9.163	111.920	27.9	5.3
2	Blitar	19-06-2008	-10.530	111.850	37.6	4.8
3	Blitar	09-07-2008	-9.000	112.480	20.0	5.0
4	Tasikmalaya	11-07-2008	-9.370	107.610	17.8	5.3

NO	Earthquake	Date	Lat.	Lon.	H (km)	M
5	Wonosari-DIY	25-08-2008	-8.720	110.810	10.0	5.3
6	Ujungkulon	26-08-2008	-6.570	104.490	37.9	5.7
7	Cilacap	09-10-2008	-9.730	108.060	38.6	5.2
8	Nusa Dua-Bali	21-10-2008	-11.710	116.020	10.0	5.0
9	Ujung Kulon	27-03-2009	-7.250	105.980	41.1	5.0
10	Tasikmalaya	14-06-2009	-8.200	107.560	19.8	5.3
11	Ujung Kulon	24-06-2009	-7.250	104.800	30.0	5.2
12	Ujung Kulon	24-06-2009	-7.140	104.750	30.0	4.9
13	Cilacap	31-07-2009	-9.210	108.680	28.3	5.4
14	Wonosari-DIY	07-09-2009	-10.330	110.620	36.1	6.2
15	Nusa Dua-Bali	18-09-2009	-9.670	115.490	36.0	6.7
16	Tasikmalaya	18-11-2009	-9.150	107.580	34.3	5.2
17	Nusa Dua-Bali	11-02-2010	-10.110	113.850	49.7	5.8
18	Ujung Kulon	03-03-2010	-7.390	104.700	30.0	5.2

NO	Earthquake	Date	Lat.	Lon.	H (km)	M
19	Cilacap	04-06-2010	-9.770	108.060	33.3	5.5
20	Cilacap	04-06-2010	-9.720	108.080	39.1	5.1
21	Wonosari-DIY	18-06-2010	-8.930	111.200	49.3	5.2
22	Blitar	26-07-2010	-10.300	112.090	22.0	4.8
23	Ujung Kulon	02-08-2010	-6.900	104.560	46.3	5.1
24	Ujung Kulon	14-08-2010	-7.470	105.890	35.0	4.9
25	Nusa Dua-Bali	01-10-2010	-11.230	113.660	47.2	5.3
26	Ujung Kulon	03-10-2010	-6.830	104.860	34.8	5.1
27	Ujung Kulon	20-11-2010	-7.470	106.040	45.8	5.2
28	Sukabumi	29-11-2010	-8.410	106.820	45.9	5.2
29	Cilacap	06-12-2010	-11.040	107.350	33.0	5.5
30	Bantul	11-12-2010	-9.920	109.540	36.0	5.4
31	Jember	03-01-2011	-10.470	113.330	23.0	5.6
32	Ujungkulon	06-02-2011	-8.400	103.860	10.0	5.7

NO	Earthquake	Date	Lat.	Lon.	H (km)	M
33	Banyuwangi	23-03-2011	-9.440	114.030	47.0	5.0
34	Cilacap	03-04-2011	-10.010	107.690	20.6	6.7
35	Cilacap	13-05-2011	-9.930	107.600	17.2	5.2
36	Blitar	17-05-2011	-9.550	112.550	40.6	5.7
37	Cilacap	28-05-2011	-8.750	108.640	45.3	5.2
38	Jember	29-06-2011	-9.650	113.720	26.0	5.3
39	Nusa Dua-Bali	13-10-2011	-9.760	114.530	35.0	5.2
40	Nusa Dua-Bali	13-10-2011	-9.890	114.530	39.0	6.2
41	Ujung Kulon	04-11-2011	-7.090	103.720	10.0	5.7
42	Nusa Dua-Bali	18-11-2011	-10.750	113.690	40.0	5.7
43	Wonosari-DIY	02-12-2011	-10.910	111.010	10.0	5.0
44	Tasikmalaya	22-12-2011	-9.120	107.740	40.7	5.2
45	Garut	15-02-2012	-7.980	107.480	10.0	5.7
46	Bandung	29-02-2012	-7.700	106.250	45.4	6.2

NO	Earthquake	Date	Lat.	Lon.	H (km)	M
47	Pandeglang-Banten	14-04-2012	-7.170	105.130	41.1	5.8
48	Pandeglang-Banten	30-04-2012	-8.240	105.480	18.7	5.0
49	Bantul-DIY	22-08-2012	-11.610	109.450	29.0	5.3
50	Banyuwangi	03-09-2012	-11.070	113.860	17.2	6.3
51	Banyuwangi	04-09-2012	-11.010	113.780	10.0	5.1
52	Banyuwangi	04-09-2012	-11.010	113.910	10.0	5.1
53	Banyuwangi	04-09-2012	-10.990	113.800	14.1	5.3
54	Banyuwangi	05-09-2012	-10.990	113.830	18.9	5.0
55	Banyuwangi	07-09-2012	-10.680	113.810	48.0	5.0
56	Banyuwangi	11-09-2012	-10.900	113.700	10.0	5.0
57	Banyuwangi	13-09-2012	-10.830	113.700	10.0	5.0
58	Banyuwangi	15-09-2012	-10.820	113.830	10.0	5.7
59	Banyuwangi	15-09-2012	-10.820	113.830	10.0	5.1
60	Banyuwangi	16-09-2012	-10.800	113.750	18.3	5.2

NO	Earthquake	Date	Lat.	Lon.	H (km)	M
61	Sukabumi	10-11-2012	-7.790	106.520	49.5	5.0
62	Ciamis	19-11-2012	-9.590	108.190	10.0	5.8
63	Pacitan	18-12-2012	-9.150	111.290	16.0	5.3
64	Pandeglang-Banten	30-12-2012	-7.010	105.200	48.3	5.0
65	Pandeglang-Banten	02-02-2013	-7.210	105.290	34.9	5.0
In-slab Earthquakes						
1	Sukabumi	23-05-2008	-8.060	106.710	66.0	4.9
2	Lumajang	12-06-2008	-9.450	112.780	53.4	5.5
3	Cilacap	18-06-2008	-8.100	107.900	94.0	4.7
4	Tasikmalaya	07-07-2008	-8.290	107.870	74.5	4.8
5	Wonosari-DIY	12-07-2008	-8.960	110.450	80.0	4.8
6	Wonogiri	20-07-2008	-9.000	111.240	88.0	5.3
7	Tasikmalaya	08-08-2008	-8.440	107.470	83.5	5.2
8	Wonosari-DIY	20-08-2008	-8.720	110.810	94.7	5.1

NO	Earthquake	Date	Lat.	Lon.	H (km)	M
9	Tasikmalaya	10-09-2008	-8.100	107.960	90.6	4.7
10	Sukabumi	26-10-2008	-7.870	107.230	84.4	5.2
11	Cilacap	17-06-2009	-8.110	108.580	75.2	5.3
12	Blitar	28-07-2009	-8.880	112.480	76.1	5.5
13	Tasikmalaya	02-09-2009	-8.120	107.330	57.8	7.0
14	Tasikmalaya	12-10-2009	-8.240	107.390	70.2	5.5
15	Sukabumi	24-10-2009	-7.470	106.380	50.4	5.2
16	Wonosari-DIY	19-11-2009	-8.920	110.450	75.1	4.9
17	Tasikmalaya	10-01-2010	-8.020	107.910	70.8	5.3
18	Wonosari-DIY	10-02-2010	-9.420	111.130	61.0	4.9
19	Ujung Kulon	20-02-2010	-7.570	105.890	51.4	5.3
20	Tasikmalaya	27-04-2010	-8.360	107.820	55.0	4.9
21	Sukabumi	18-05-2010	-8.220	107.210	71.3	5.3
22	Lumajang	21-05-2010	-9.540	112.840	50.8	5.2

NO	Earthquake	Date	Lat.	Lon.	H (km)	M
23	Jember	26-05-2010	-9.510	113.570	66.5	5.3
24	Blitar	06-06-2010	-9.380	112.420	79.0	5.3
25	Tasikmalaya	26-06-2010	-8.370	107.980	100.0	5.9
26	Sukabumi	11-08-2010	-8.050	106.910	55.3	5.3
27	Malang	16-08-2010	-8.800	112.530	68.3	5.2
28	Tasikmalaya	19-08-2010	-9.420	107.020	68.3	5.5
29	Sukabumi	14-10-2010	-7.880	106.410	50.4	5.2
30	Ujung Kulon	04-11-2010	-7.970	104.670	50.0	5.2
31	Sukabumi	09-11-2010	-8.980	110.080	56.8	5.1
32	Bantul	09-11-2010	-8.150	107.150	57.2	6.0
33	Wonosari-DIY	21-12-2010	-9.080	111.190	59.9	5.5
34	Ujung Kulon	12-01-2011	-7.210	105.150	50.2	5.0
35	Jember	08-02-2011	-10.370	113.790	50.0	5.2
36	Jember	14-02-2011	-10.080	113.750	58.7	5.2

NO	Earthquake	Date	Lat.	Lon.	H (km)	M
37	Sukabumi	20-03-2011	-7.930	106.790	58.1	4.9
38	Ujung Kulon	04-04-2011	-7.380	105.970	55.1	5.2
39	Cilacap	26-04-2011	-8.600	108.360	81.5	5.6
40	Blitar	18-05-2011	-9.440	112.560	62.8	5.2
41	Cilacap	01-07-2011	-8.730	108.660	92.9	5.3
42	Sukabumi	24-07-2011	-7.520	106.430	59.1	5.0
43	Sukabumi	21-08-2011	-7.570	106.640	78.9	5.0
44	Jember	23-01-2012	-9.760	113.310	56.8	5.5
45	Jember	28-03-2012	-9.360	113.470	52.1	5.0
46	Cianjur	12-04-2012	-7.990	107.060	57.6	5.7
47	Tasikmalaya	20-05-2012	-8.280	107.950	65.9	5.5
48	Sukabumi	04-06-2012	-7.990	106.190	50.0	5.8
49	Cianjur	27-06-2012	-7.680	107.140	86.6	5.5
50	Kebumen	13-07-2012	-8.370	109.020	74.3	5.3

NO	Earthquake	Date	Lat.	Lon.	H (km)	M
51	Banyuwangi	18-09-2012	-10.910	113.970	114.0	5.2
52	Pandeglang-Banten	14-12-2012	-7.780	105.690	75.5	5.0
53	Pandeglang-Banten	11-02-2013	-7.030	105.230	54.0	4.5

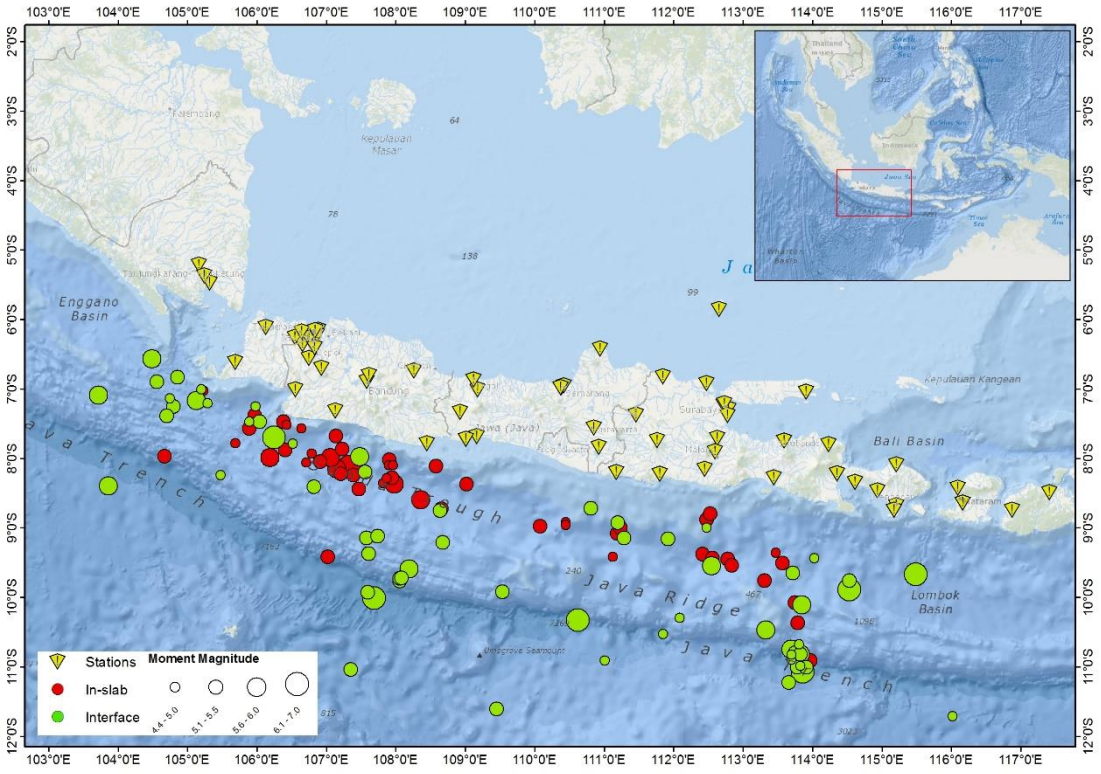

Figure 6 Locations of analyzed earthquakes and recording stations.

Scrodilis (2006) defined the empirical relations for converting M_S, m_b, and M_L magnitudes to **M**. Scrodilis (2006) used a very large sample of data from international seismological sources, e.g., the International Seismological Centre (ISC), the National Earthquake Information Centre (NEIC), the Global Centroid Moment Tensor database (known as the Havard [HVRD] or GCMT Catalog) and the United States Geological

Survey (USGS). The database contains 20,407 events that occurred over the world during the time period of 1976 to 2003.

The ISC and the NEIC released body wave magnitude as m_B and m_b. Abe (1981) proposed the empirical relationship between m_B and m_b as the following equation:

$$m_B = 1.5m_b - 2.2 \quad (3.1)$$

Then to connect m_b estimated by NEIC to m_b estimated by ISC, Scordilis (2006) proposed the following relation:

$$m_{b,ISC} = 1.02m_{b,NEIC} - 0.18, \quad (3.2)$$

with $2.5 \leq m_{b,NEIC} \leq 7.3$ and $R^2 = 0.99$. This equation showed that the m_b given by the ISC and the NEIC are, practically, equivalent.

The estimation of **M** (released by the Harvard CMT catalog) from m_b estimated by Equation (3.2) is performed by using the following relation (Scordilis, 2006):

$$\mathbf{M} = 0.85m_b + 1.03 \quad (3.3)$$

For converting the local magnitude (M_L) estimated by the ISC, it cannot be considered as equivalent due to impossibility of defining the unique global relations connecting M_L to other magnitude scales. For this reason, specific regional relations are required (Scrodilis, 2006). Irsyam et al. (2010) have provided the relationship for the Indonesia region between M_L and mb as given by:

$$m_b = 0.125M_L^2 - 0.389M_L + 3.513 \quad (3.4)$$

By using this equation and Equation (3.3), the M_L magnitude scales are converted to **M**.

3.5 Source to Site Distance

Source-to-site distances are used to describe the decreasing of ground motion in terms of both anelastic attenuation and geometric, as it propagates away from the source of the earthquake. Different seismologists used different source-to-site distance measures. There are several distance measures used in the GMPEs: R_{jb}, is known as the "Joyner-Boore distance" is the closest horizontal distance to the vertical projection of the fault rupture plane; R_{rup}, is the closest distance to the fault rupture plane; R_{seis}, is the closest distance to the seismogenic part of the fault rupture plane; R_{hypo}, is the hypocentral distance (Abrahamson and Shedlock, 1997). The hypocentral distance is the distance between the epicenter (R_{epi}) and its focal point (the exact point where earthquake occurred, i.e., depth: h_{hypo}). These different distance measurements are schematically shown in Figure 7.

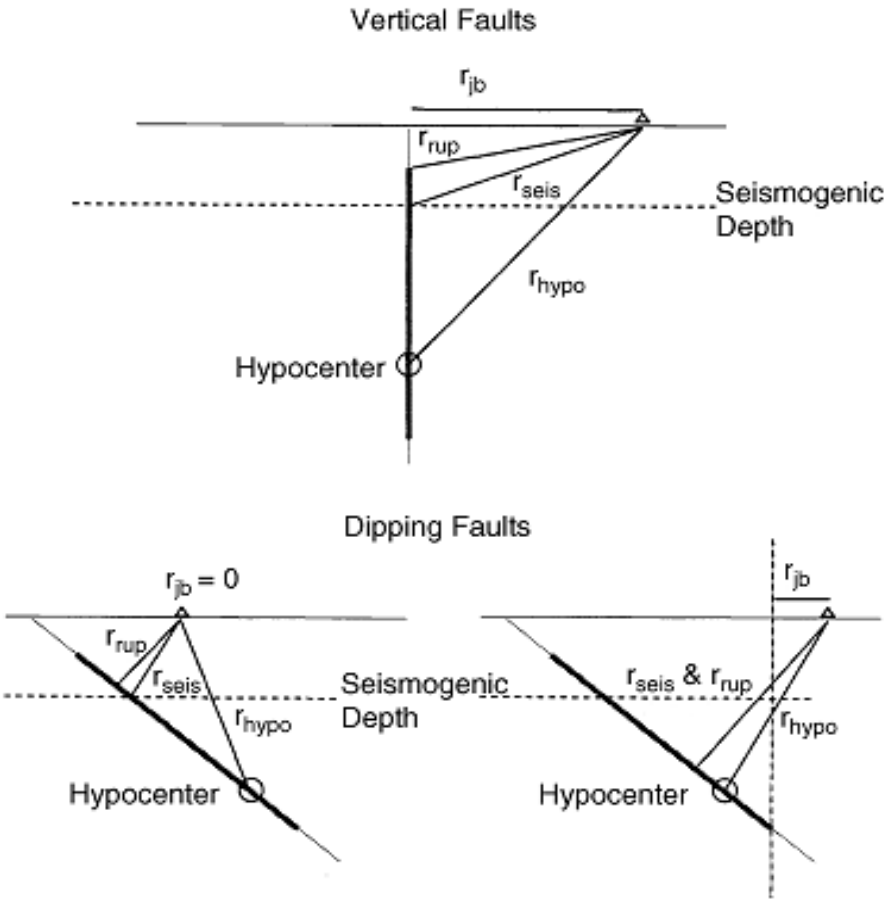

Figure 7 Comparison graphically between distance measures used in development of GMPEs (Abrahamson and Shedlock, 1997).

To calculate R_{seis} and R_{rup} is not a simple task. We need firstly to understand the rupture-specific information. If the information of rupture-specific is not available, we can calculate the average depth to the top of the fault rupture plane or to the seismogenic part using the equation from Campbell (2000b), and the size of the fault plane can be determined by the empirical relationships proposed by Wells and Coppersmith (1994) that predict fault length and area as a function of moment magnitude. The source-to-site distance parameter used in this study is the rupture distance (R_{rup}). The empirical

relationships developed by Wells and Coppersmith (1994) used to calculate the rupture length for all slip types is given by

$$\text{Log}_{10}\, L = -3.22 + 0.69\, \mathbf{M} \qquad (3.5)$$

While the equation used to calculate the fault rupture width for all slip types is given by

$$\text{Log}_{10}\, W = -1.01 + 0.32\, \mathbf{M} \qquad (3.5)$$

Figure 8 describes the geometry of a fault.

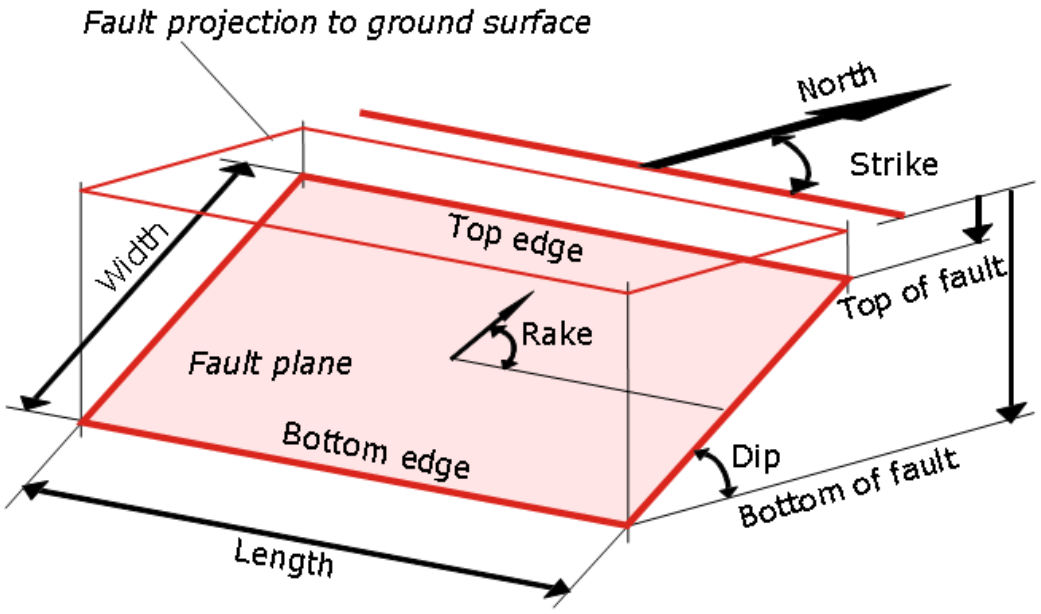

Figure 8 Fault geometry used in earthquake study.

3.6 Local Site Conditions

Propagation of seismic waves from the bedrock to the ground surface causes the earthquake shaking alteration. It is affected by local site conditions that describe the type

of deposits that lie beneath the site. They are commonly described in terms of surface geology, shear-wave velocity, thickness, elasticity, and ground water level. Local site conditions have been traditionally classified into two types: soil and rock. I classified the local site conditions according to definitions of the National earthquake Hazard Reduction Program (NEHRP) site categories. Depending on the 2009 edition of the International Building Code (IBC) and also used in the Indonesian Earthquake Resistant Building Code (SNI 1726-2012), the 30-m average shear-wave velocity (V_S^{30}) is the main basis for classifying the NEHRP site class. These classifications are reproduced in Table 2.

The 30-m V_s data were provided by the BMKG for some locations. For the other locations that are not available, I estimated the site conditions from the Global V_s^{30} Map Server on the USGS website. Wald and Allen (2007) described a methodology for deriving site-conditions anywhere in the world using topographic slope as a proxy. The estimated site conditions from the Global V_s^{30} Map Server for Java Island is shown in Figure 9.

Table 2 NEHRP site classifications based on shear-wave velocity.

NEHRP Site Class		V_s^{30}
Soil Profile Name	**Code**	
Hard rock	A	≥1500
Rock	B	750-1500
Very dense soil and soft rock	C	350-750
Stiff soil	D	175-350
Soft soil	E	<175

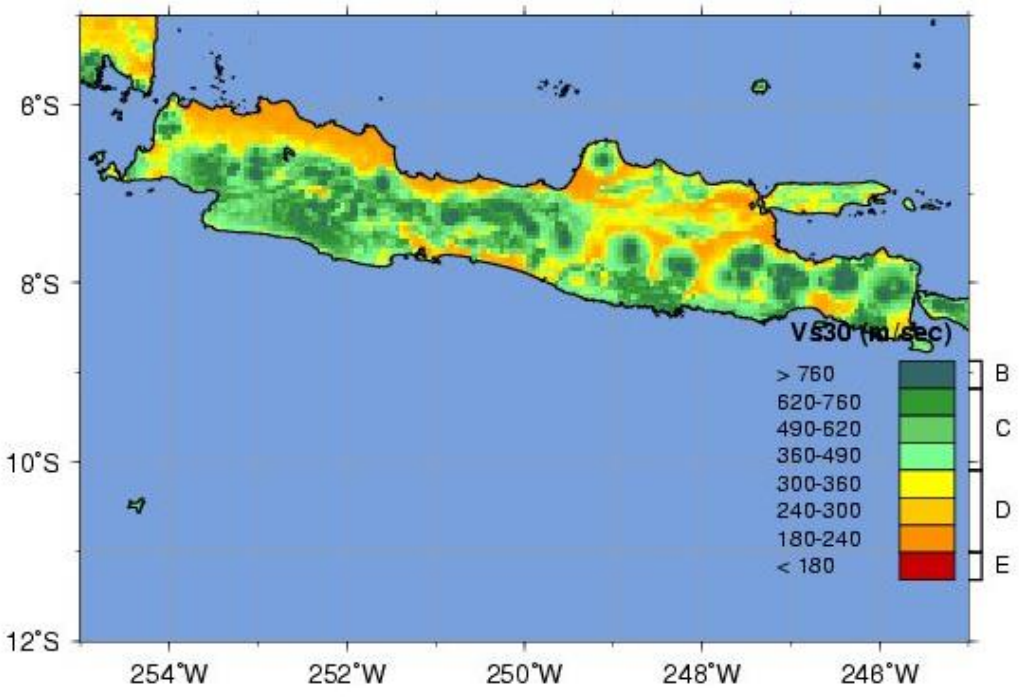

Figure 9 The estimated site conditions for Java Island from the Global V_s^{30} Map Server (USGS).

Moreover, ground shaking on surface will generally display amplification. The amplification factor is defined as the ratio of the magnitude of PGA or PSA at the surface divided by the PGA or PSA at bedrock. The amplification factor has different values and depends on site classifications. The 2010 edition of the American Society of Civil Engineers (ASCE) released the amplification factor for PGA, short period, and long period depending on site classifications as well as that followed by the Indonesian Earthquake Resistant Building Code (SNI 1726-2012). Table 2 lists the amplification factor for PGA.

Table 3 Amplification factor for peak ground acceleration (PGA) depending on ASCE-7 (2010) and SNI-1726 (2012).

Site Class	Amplification Factor for PGA (in g)				
	PGA ≤ 0.1	**PGA = 0.2**	**PGA = 0.3**	**PGA = 0.4**	**PGA ≥ 0.5**
A	0.8	0.8	0.8	0.8	0.8
B	1.0	1.0	1.0	1.0	1.0
C	1.2	1.2	1.1	1.0	1.0
D	1.6	1.4	1.2	1.1	1.0
E	2.5	1.7	1.2	0.9	0.9

CHAPTER 4

DATA ANALYSIS

4.1 Overview

To develope GMPEs for subduction zone earthquakes, I need to subdivide the database into two types: interface and in-slab earthquakes. Interface earthquakes can be defined as shallow angle thrust events that occur at the interface between the subducting and overriding plates. In-slab earthquakes are typically high-angle normal-faulting events responding to down-dip tension in the subducting plate and occur within the subducting oceanic plate (Youngs *et al.*, 1997). Thrust mechanisms indicate that interface earthquakes occur at depth of less than 50 km and in-slab earthquakes occur at depth greater than 50 km (Tichelaar and Ruff, 1993). The list of both interface and in-slab earthquakes can be seen in Table 1 in Section 3.4.

4.2 Data Sources

The dataset compiled for all available ground motion recordings (accelerograph stations) from the Indonesian-Meteorological Climatological and Geophysical Agency

(BMKG) and recorded from March 2008 to February 2013, contains 3,148 horizontal-component spectra subdivided to; 1,810 from interface earthquakes and 1,338 from in-slab earthquakes. All data obtained from accelerograph stations consist of ground motion on surface. To obtain ground motions on rock (NEHRP B), I divided the data by an amplification factor as explained in Section 3.6. Figure 10 shows the distribution of the database used in the regression analysis with respect to **M** for interface earthquakes, while Figure 11 shows that of in-slab earthquakes. Figure 12 shows the data distribution with respect to PGA for interface events, while Figure 13 shows that of in-slab events.

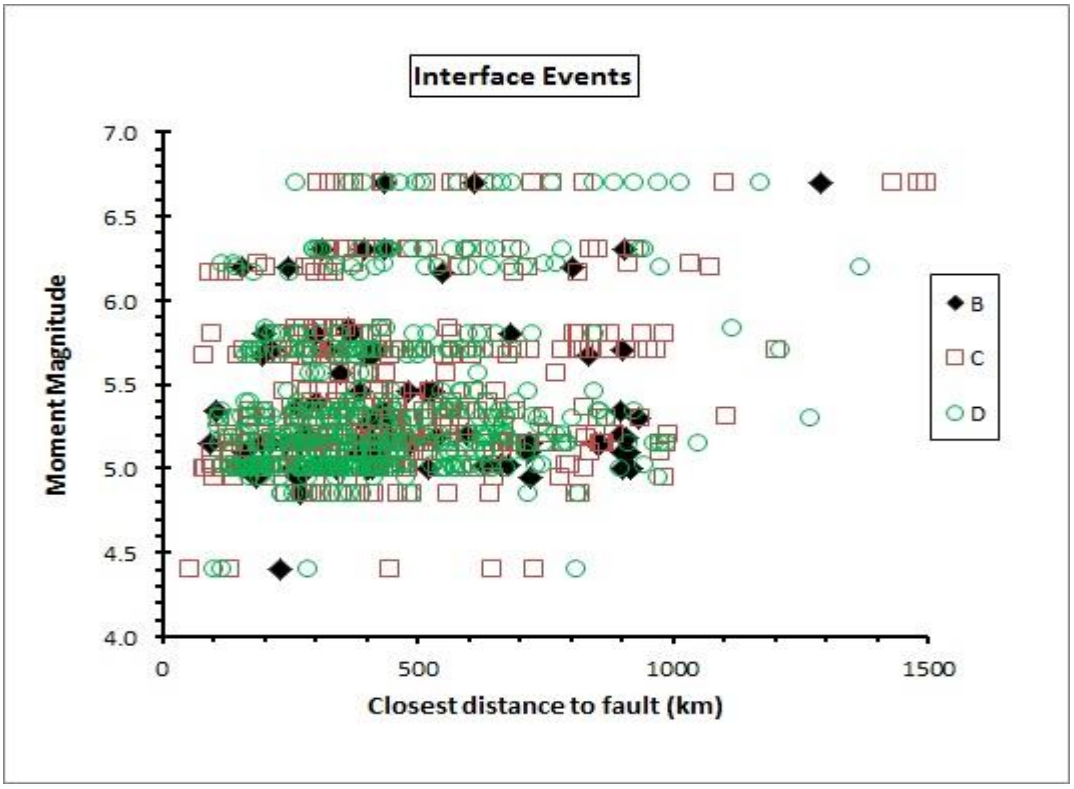

Figure 10 Dataset distribution with respect to moment magnitude for interface events, by NEHRP site class.

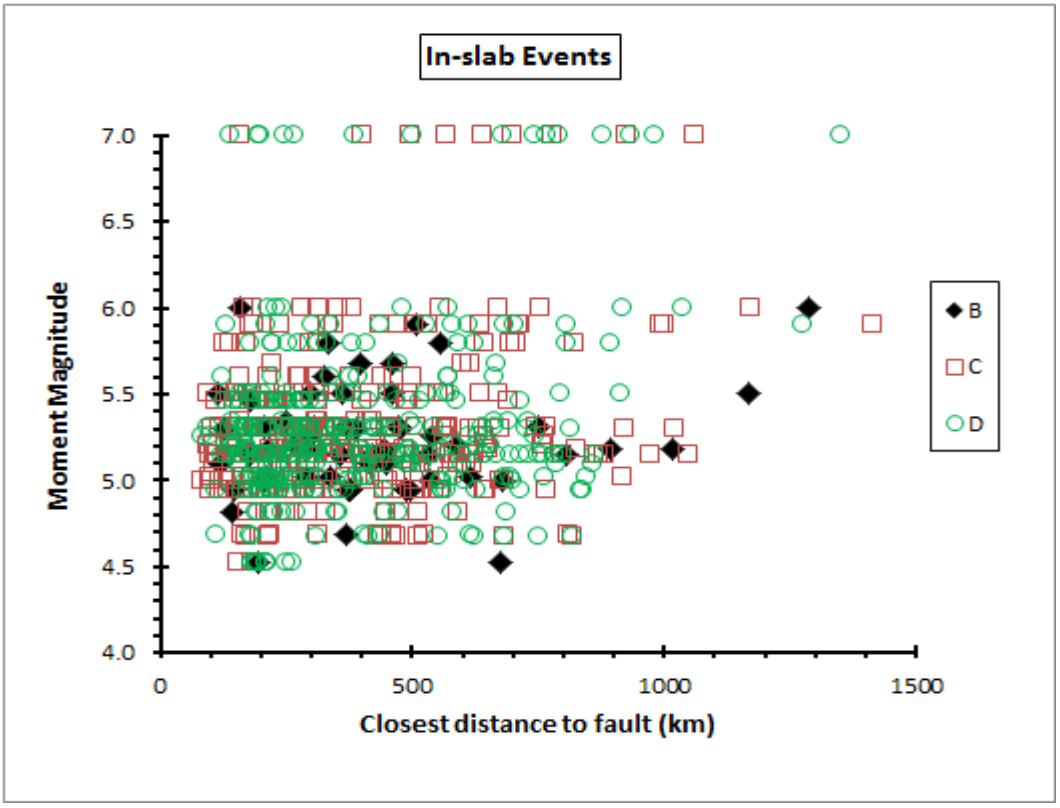

Figure 11 Dataset distribution with respect to moment magnitude for in-slab events, by NEHRP site class.

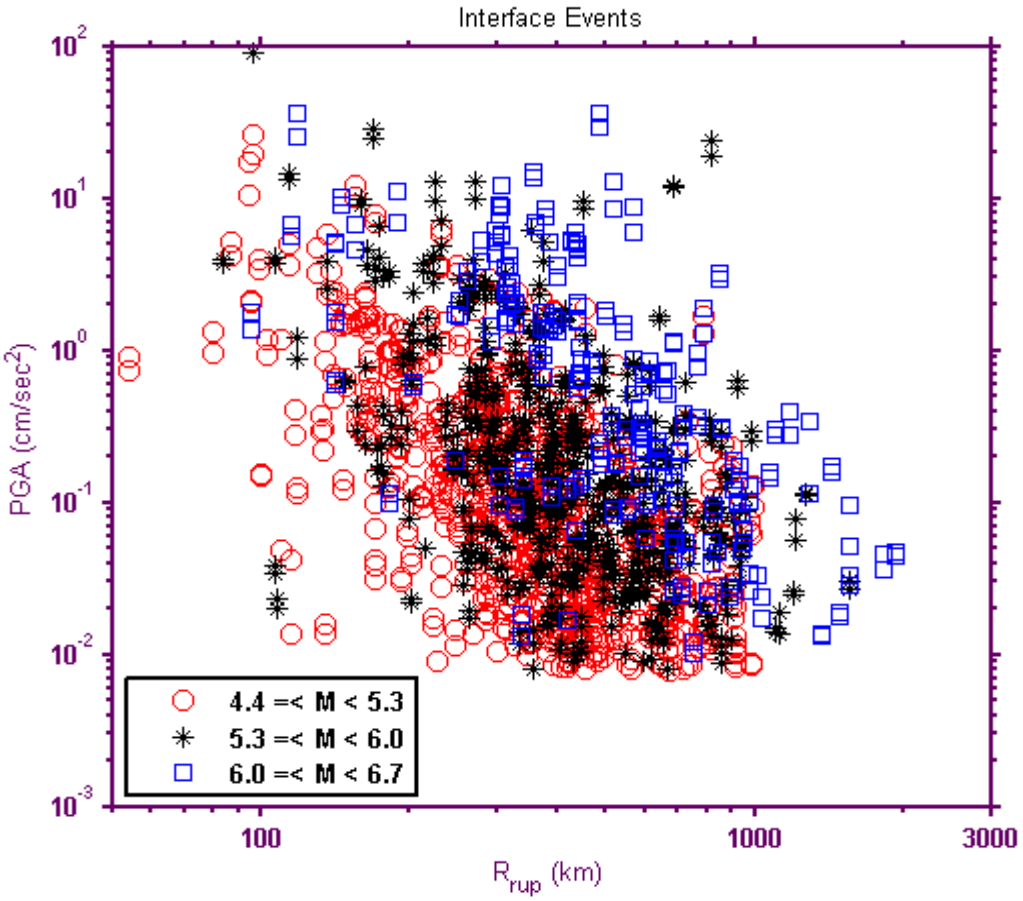

Figure 12 Dataset distribution with respect to PGA in three magnitude ranges for interface events.

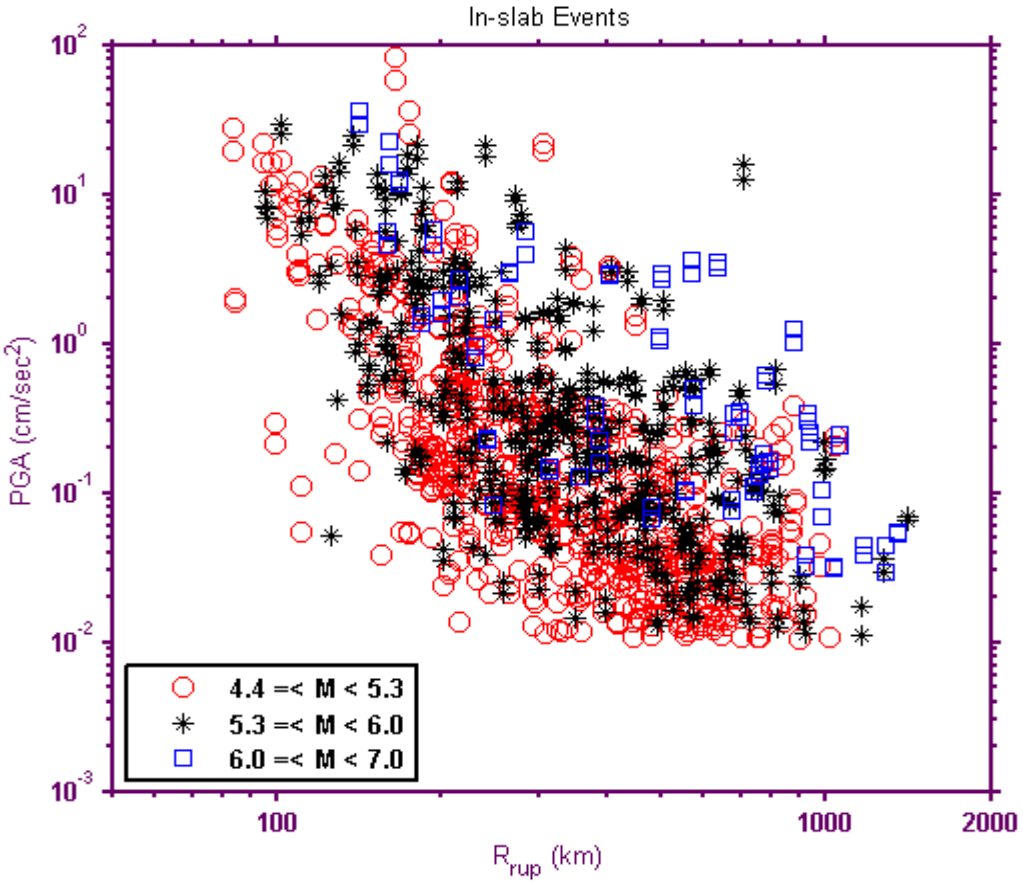

Figure 13 Dataset distribution with respect to PGA in three magnitude ranges for in-slab events.

4.3 Regression Analysis

The regression analysis of our dataset was performed using the least square method. Our functional form is

$$\text{Log}_{10}(\boldsymbol{Y}) = fn(\mathbf{M}) + C_3H + C_4R_{rup} - S^*\log_{10}(R_{rup}) \qquad (4.1)$$

Where $\boldsymbol{Y}$ is PGA of 5% damped PSA in cm/s^2 at bedrock. **M** is the moment magnitude. $fn(\mathbf{M})$ can be noticed as a linear ($fn(\mathbf{M}) = C_1 + C_2\mathbf{M}$) or a quadratic form ($fn[\mathbf{M}] = C_0' + C_1'[\mathbf{M} - 5.8] + C_2'[\mathbf{M} - 5.8]^2$). Atkinson and Boore (2003) selected the linear form. H is

focal depth in kilometers. S is the magnitude dependence of the geometric spreading coefficient, where $S = 10^{(2.6891 - 0.6804\mathbf{M})}$ for interface events and $S = 10^{(-1.5296 - 0.0297\mathbf{M})}$ for in-slab events. R_{rup} is the closest distance to the fault rupture plane in kilometers.

The S term was determined by preliminary regression of the dataset at low frequency (Atkinson and Boore, 2003), in this study I used data at 1 Hz. The regression looked at slices of data in 0.5-unit magnitude increments (e.g., $4.5 \leq \mathbf{M} \leq 5$, $4.7 \leq \mathbf{M} \leq 5.2$, etc.). For example, the value plotted at **M** 6.0 is the slope for data of $5.75 \leq \mathbf{M} \leq 6.25$. Figure 14 shows the S term obtained for both interface and in-slab events. The values of attenuation slope are from slope of $\log_{10} Y'$ versus $\log_{10} R_{rup}$ for each magnitude bin, where Y' = PSA (1 Hz) exp(0.001 R_{rup}).

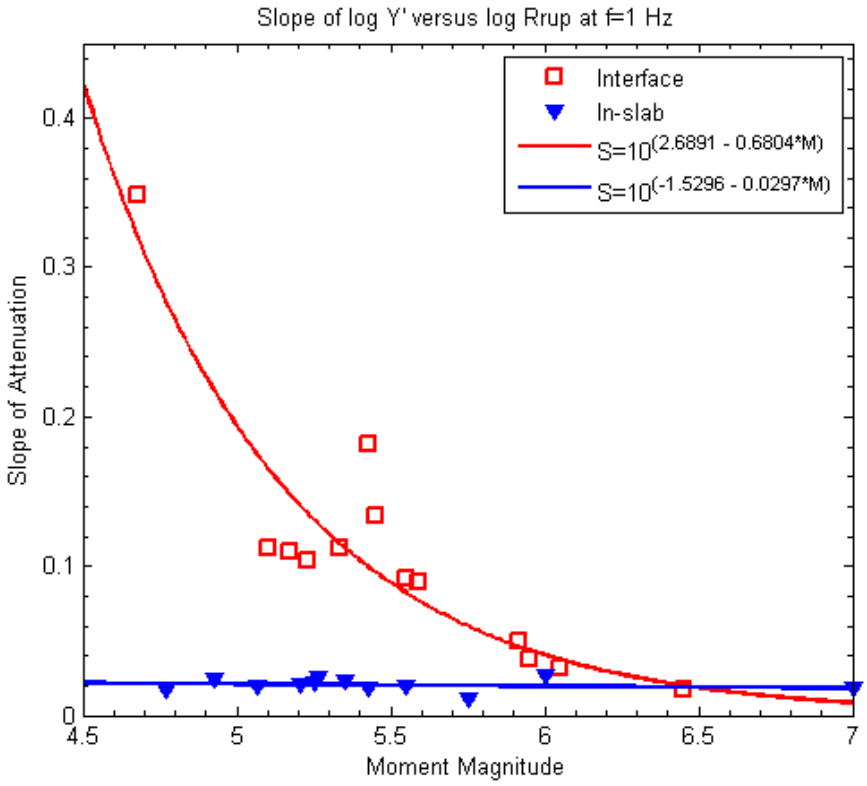

Figure 14 The magnitude dependence of the geometric spreading coefficient *S* for interface (open squares) and in-slab (filled triangles).

The *fn*(**M**) is a function relevant to the magnitude. This function can be expressed as a linear or quadratic term. For interface events, there is a big different between the quadratic term and linear term, while for in-slab events, the fitting curve is almost the same. Also the quadratic term has a better fit than the linear term, but the sign of the quadratic term is positive, rather than a negative sign as would be expected. Therefore, I selected the linear term as the final regression functions. Figure 15 and 16 show the scaling of ground motion amplitudes with moment magnitude for interface events as well as Figures 17 and 18 for in-slab events in both near and far distances.

The standard error of the regression equation is given by

$$\sigma_{log\,Y} = \sqrt{\frac{1}{n-p}\sum_{i=1}^{n}(log[predicted]_i - log[observed]_i)^2} \qquad (4.2)$$

with n is the amount of recordings and p is defined as the number of regression coefficients (Bozorgnia and Campbell, 2004).

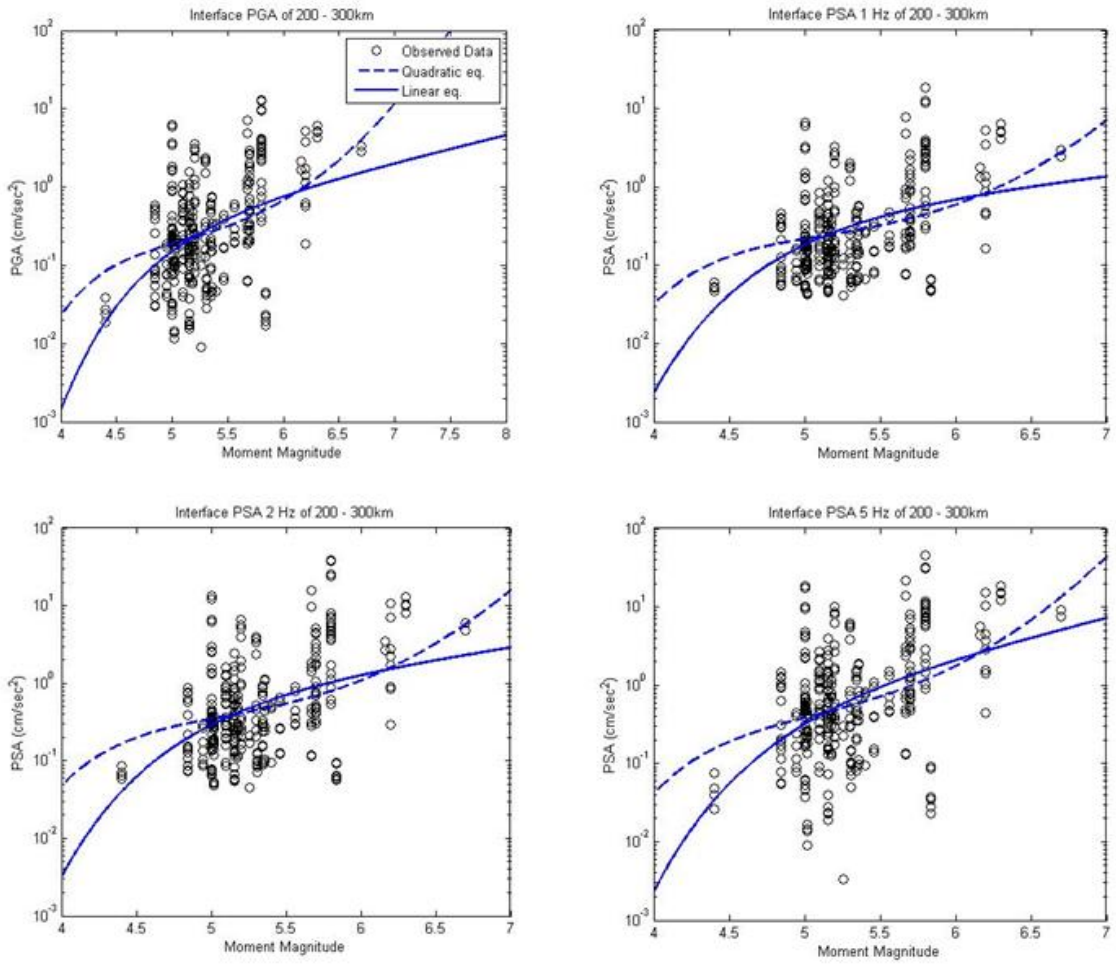

Figure 15 Scaling of ground motion amplitudes with moment magnitude for interface events in the rupture distance range from 200-300 km. I assumed that the focal depth is 25 km. Dashed lines show the scaling using the quadratic term of *fn*(M), while the solid line shows the scaling from *fn*(M) expressed linear term.

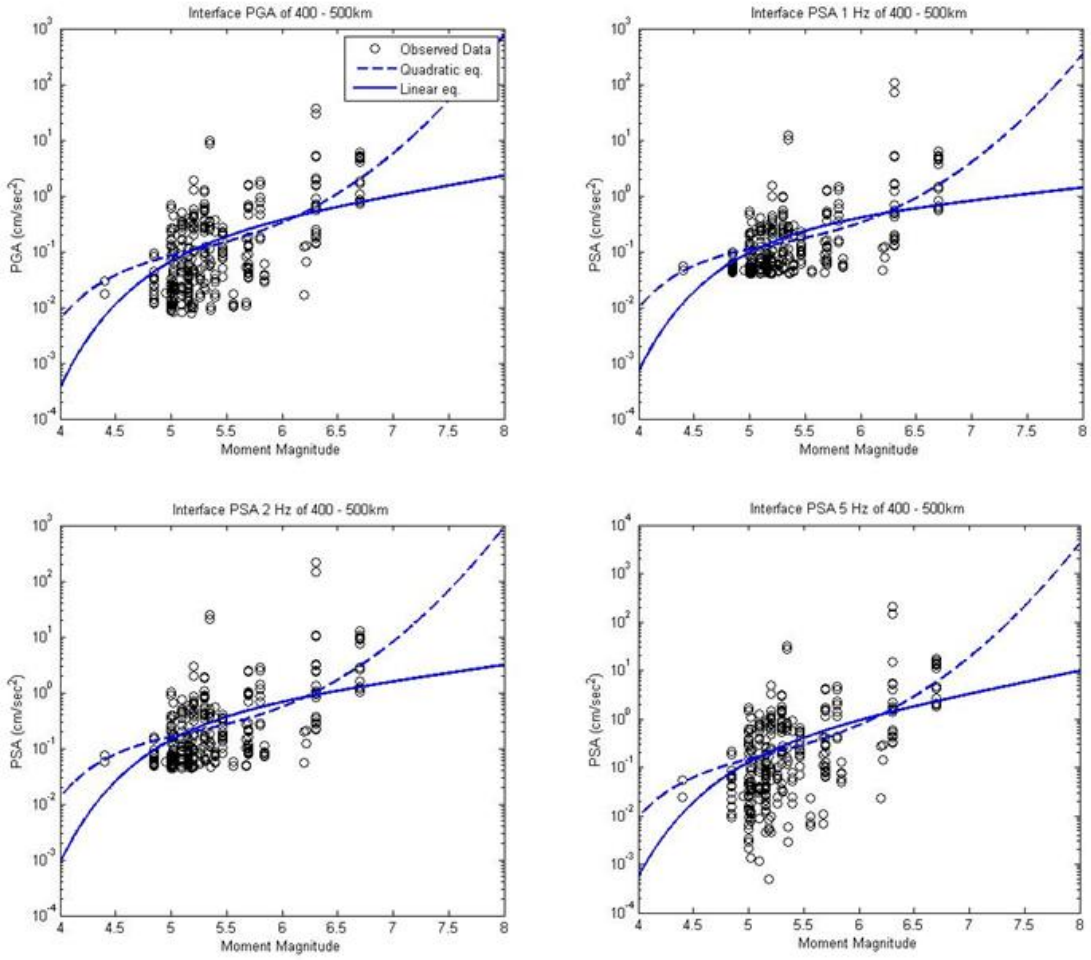

Figure 16 Scaling of ground motion amplitudes with moment magnitude for interface events in the rupture distance range from 400-500 km. I assumed that the focal depth is 25 km. Dashed lines show the scaling using the quadratic term of *fn*(M), while the solid line shows the scaling from *fn*(M) expressed linear term.

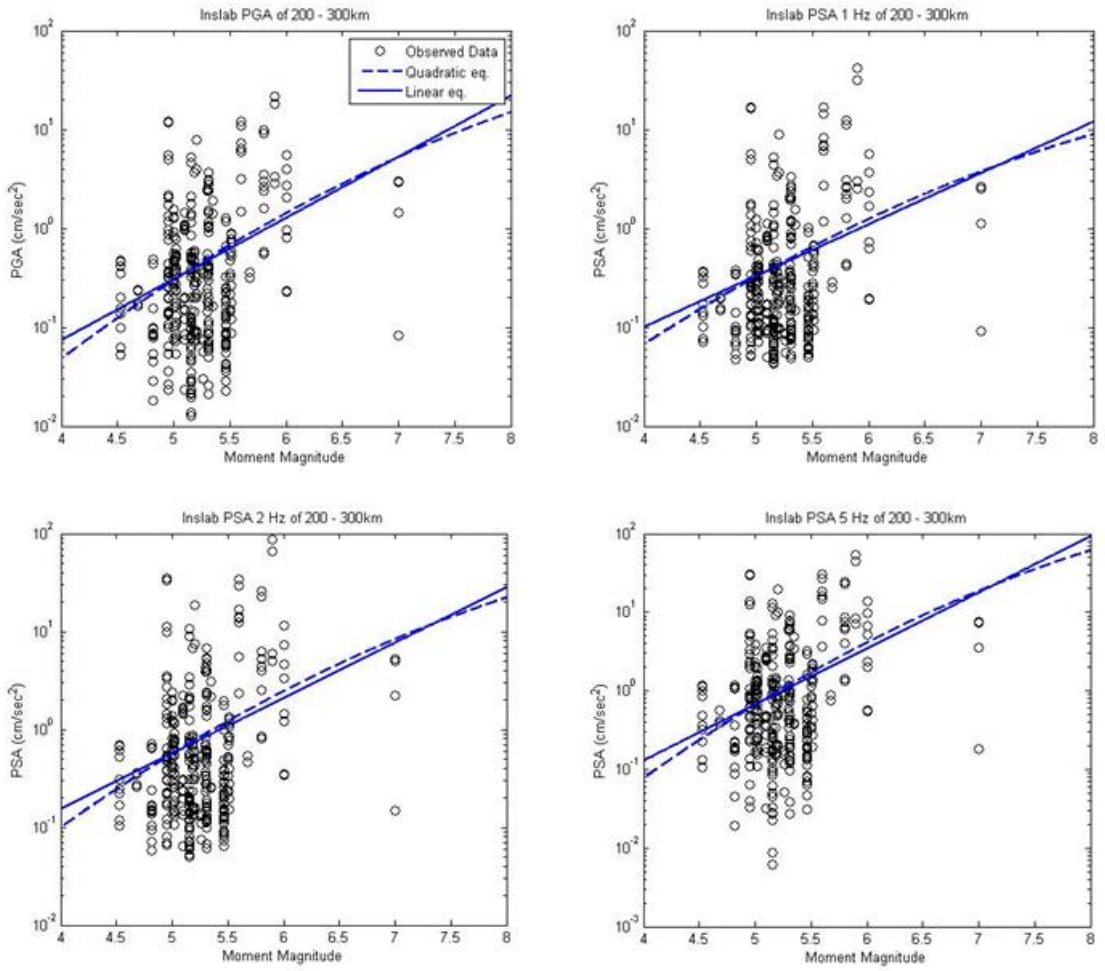

Figure 17 Scaling of ground motion amplitudes with moment magnitude for in-slab events in the rupture distance range from 200-300 km. I assumed that the focal depth is 60 km. Dashed lines show the scaling using the quadratic term of *fn*(M), while the solid line shows the scaling from *fn*(M) expressed linear term.

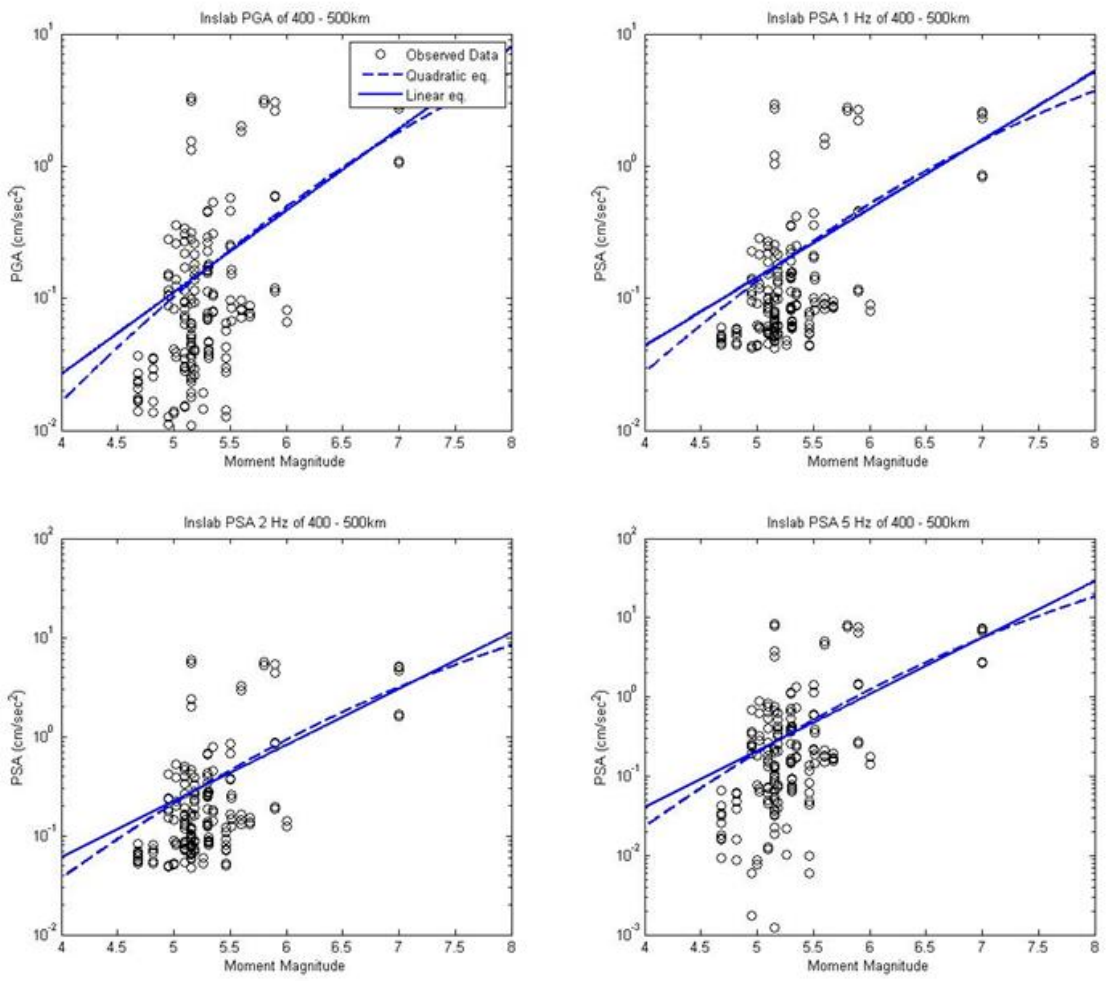

Figure 18 Scaling of ground motion amplitudes with moment magnitude for inslab events in the rupture distance range from 400-500 km. I assumed that the focal depth is 60 km. Dashed lines show the scaling using the quadratic term of *fn*(M), while the solid line shows the scaling from *fn*(M) expressed linear term.

4.4 Regression Results

The resultant coefficients for the predicted GMPEs for both interface and in-slab events are tabulated in Table 4. In interface events, the distribution of the dataset in the regression analysis covers 4.4 − 6.7 for moment magnitude, 10 − 49.7 km for focal depth, and 54 − 1,926 km for rupture distance. In in-slab events, the distribution covers 4.5 − 7.0

for moment magnitude, 50 − 100 km for focal depth, and 83 − 1,416 km for rupture distance.

Table 4 Regression Coefficients

Freq. (Hz)	C_1	C_2	C_3	C_4	C_5	C_6	$\sigma_{log\ \mathbf{Y}}$
Coefficients for Interface events							
PGA	-2.0827	0.3826	0.0055	-0.0015	2.6891	-0.6804	0.6169
1	-1.3866	0.2466	0.0046	-0.0011	2.6891	-0.6804	0.5195
2	-1.4900	0.3141	0.0051	-0.0013	2.6891	-0.6804	0.5683
5	-2.3375	0.5037	0.0062	-0.0017	2.6891	-0.6804	0.7358
Coefficients for In-slab events							
PGA	-3.1635	0.6705	-0.0026	-0.0022	-1.5296	-0.0297	0.6077
1	-2.6888	0.5618	-0.0024	-0.0018	-1.5296	-0.0297	0.5683
2	-2.6506	0.6134	-0.0027	-0.0020	-1.5296	-0.0297	0.6084
5	-3.2535	0.7732	-0.0029	-0.0025	-1.5296	-0.0297	0.6924
The regression equation is: $\mathrm{Log}_{10}(\boldsymbol{Y}) = C_1 + C_2\mathbf{M} + C_3H + C_4R_{rup} - 10^{(C5\ +\ C6\mathbf{M})}\log_{10}(R_{rup})$ with standard deviation $\sigma_{log\ \mathbf{Y}}$.							

To evaluate the performance of the regression results, I analyzed the residuals. The residuals are measured in log (base 10) units and defined as the difference between the log of observed ground-motion values and the log of predicted values. Figures 19 to 22 show the residuals for interface events as a function of distance in three magnitude ranges, while Figures 23 to 26 show the corresponding plot for in-slab events. The residuals indicate a random variability, however, overall, the majority of the average residuals are near zero for the distance range between 100 and 700 km from the fault. The residuals distributions suggest that ground-motions values can be better estimated at far-distance by the relations than those at near distance. The far-distance range is of great interest to us as the majority of infrastructure in Java Island is located at 200-300 km from the subduction zone.

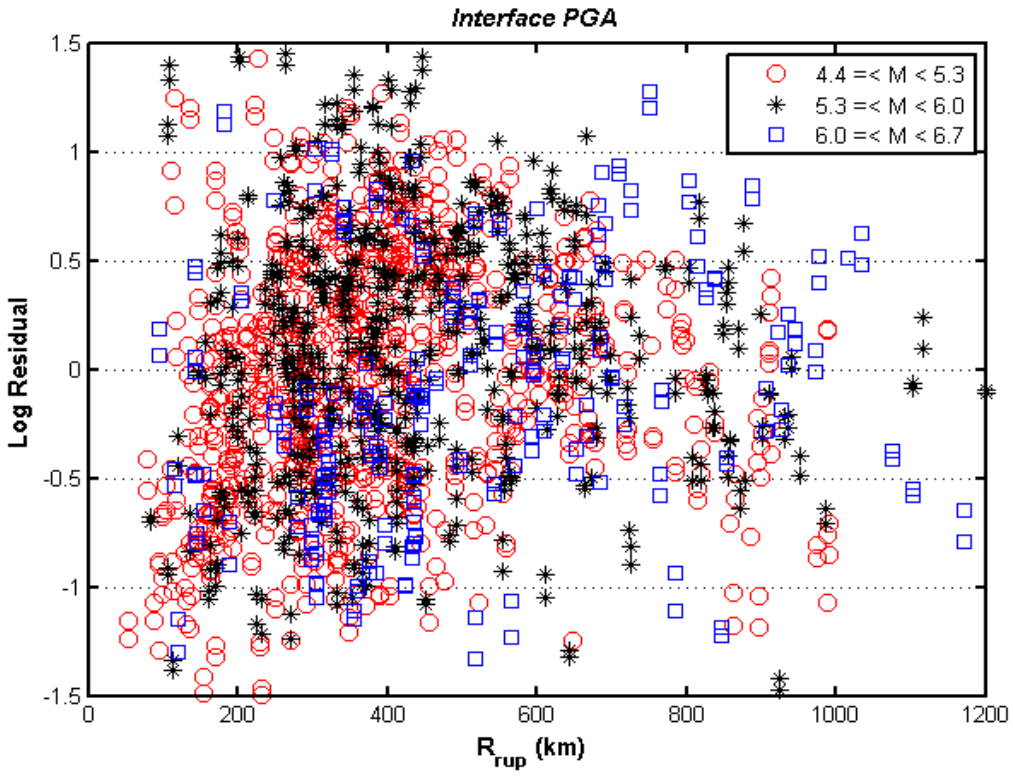

Figure 19 Distribution of log residuals with respect to rupture distance and distinguished by magnitude, for interface events at a frequency of 0 Hz (PGA).

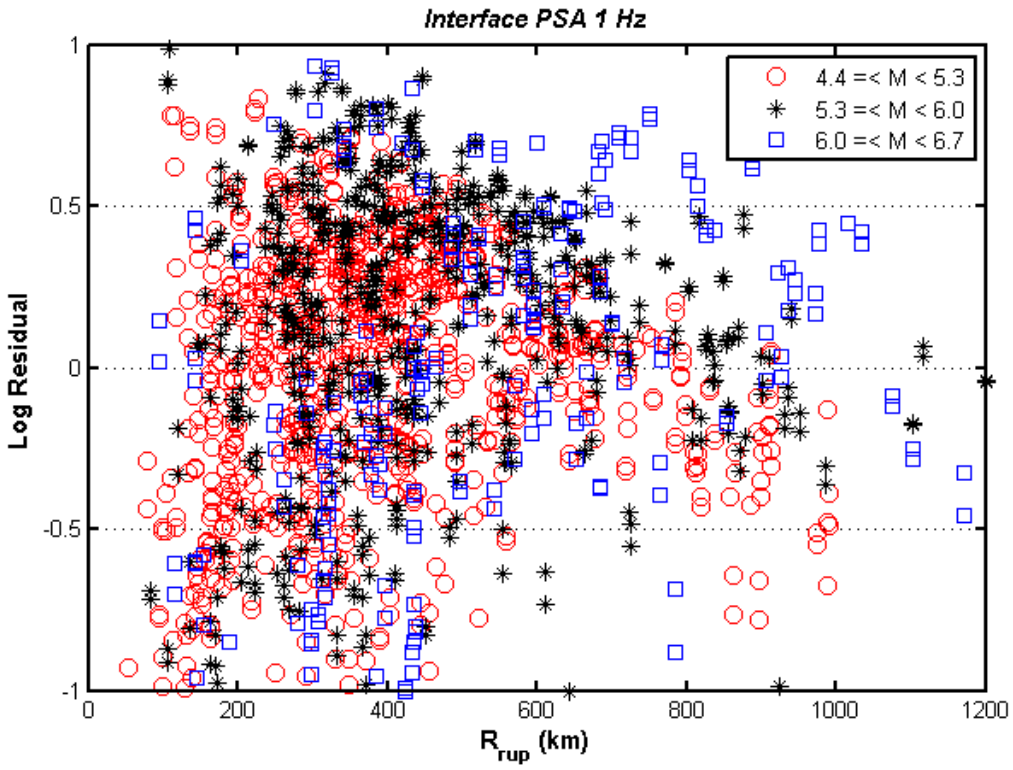

Figure 20 Distribution of log residuals with respect to rupture distance and distinguished by magnitude, for interface events at a frequency of 1 Hz.

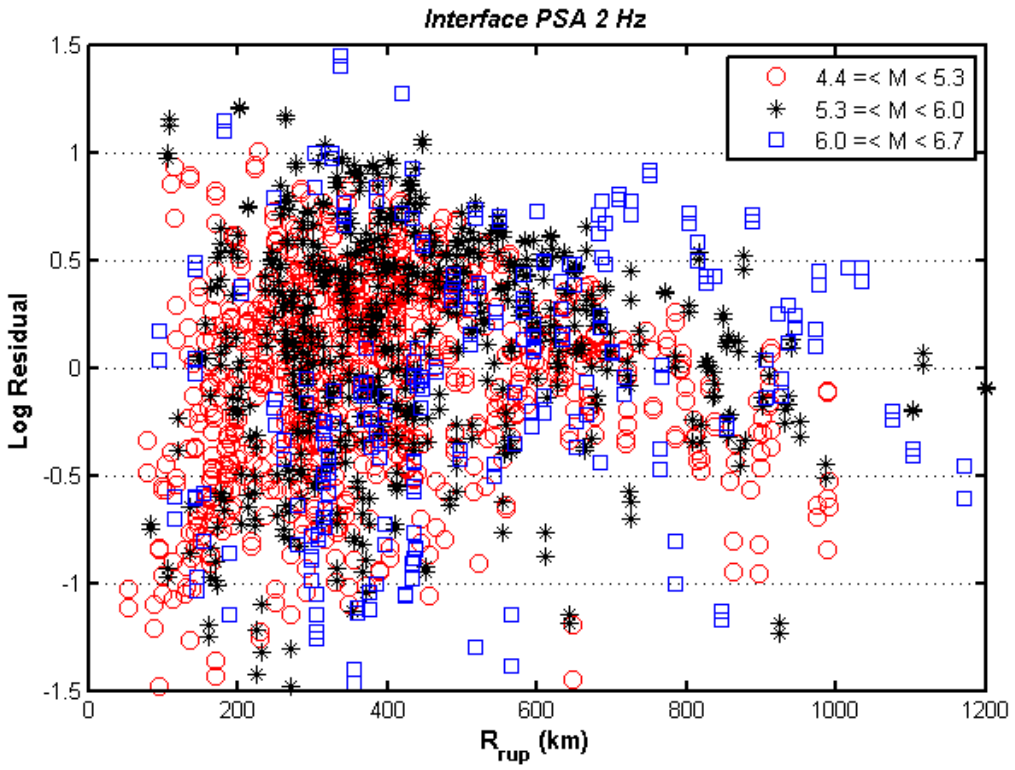

Figure 21 Distribution of log residuals with respect to rupture distance and distinguished by magnitude, for interface events at a frequency of 2 Hz.

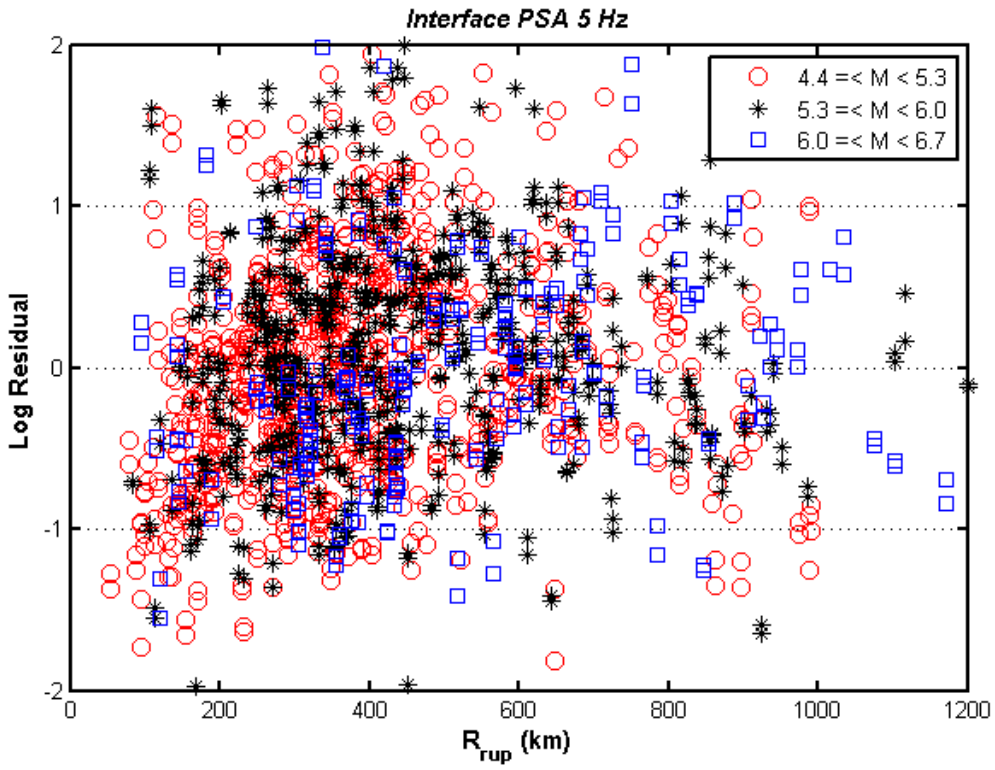

Figure 22 Distribution of log residuals with respect to rupture distance and distinguished by magnitude, for interface events at a frequency of 5 Hz.

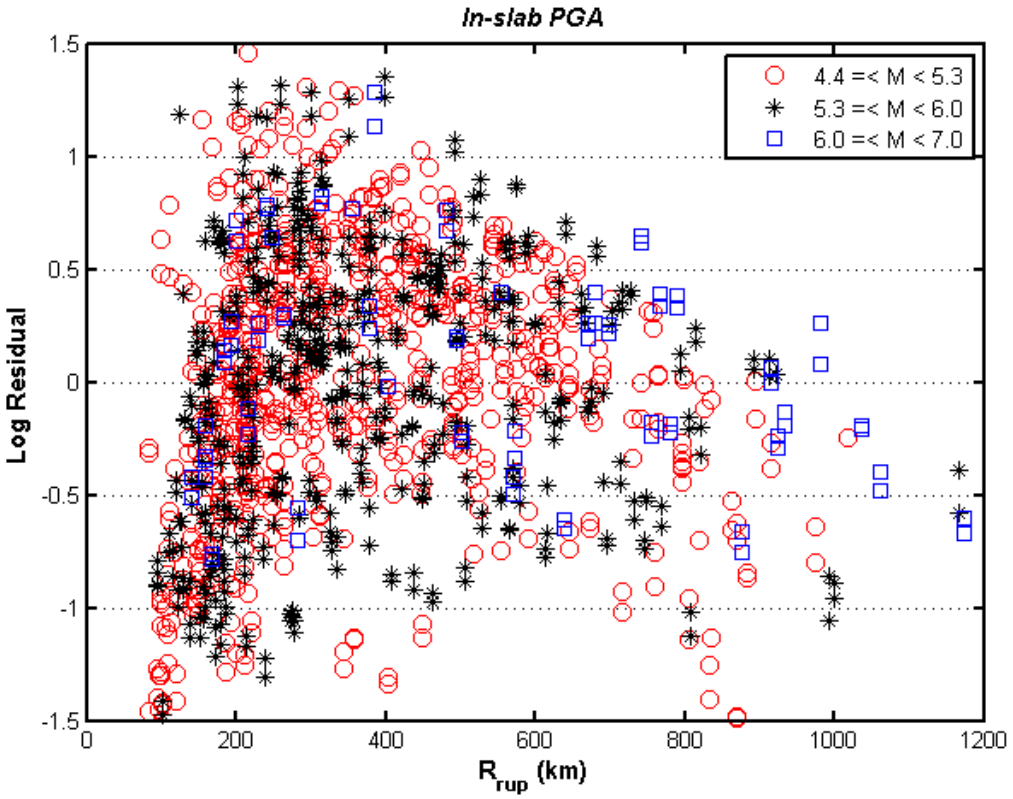

Figure 23 Distribution of log residuals with respect to rupture distance and distinguished by magnitude, for in-slab events at a frequency of 0 Hz (PGA).

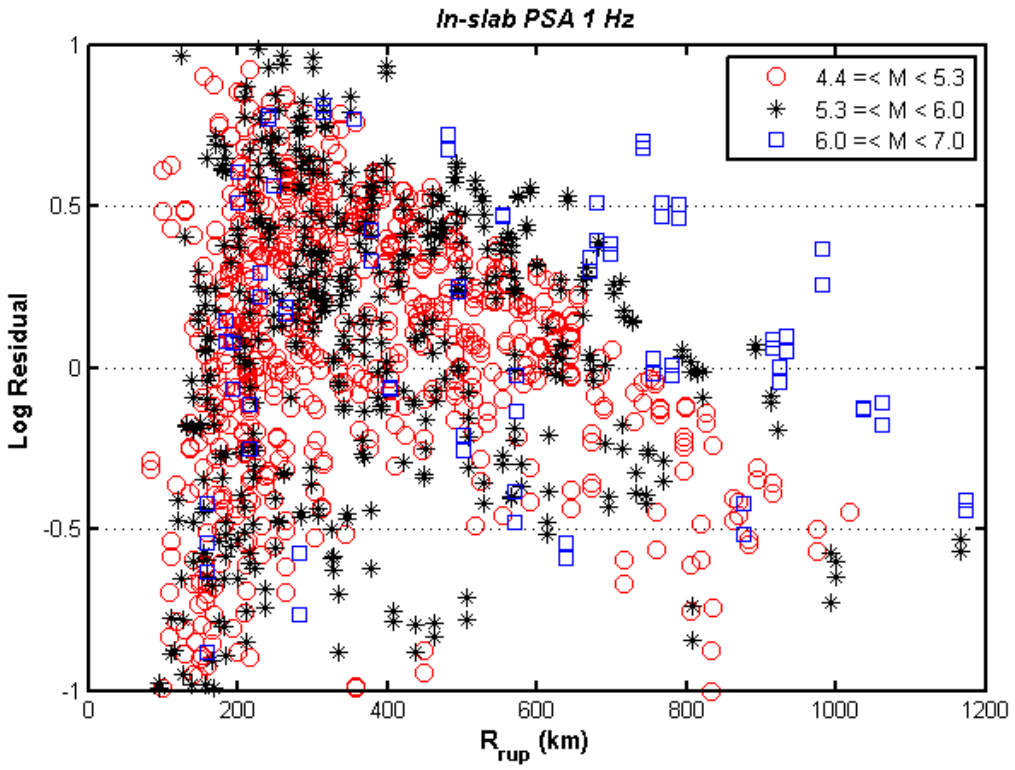

Figure 24 Distribution of log residuals with respect to rupture distance and distinguished by magnitude, for in-slab events at a frequency of 1 Hz.

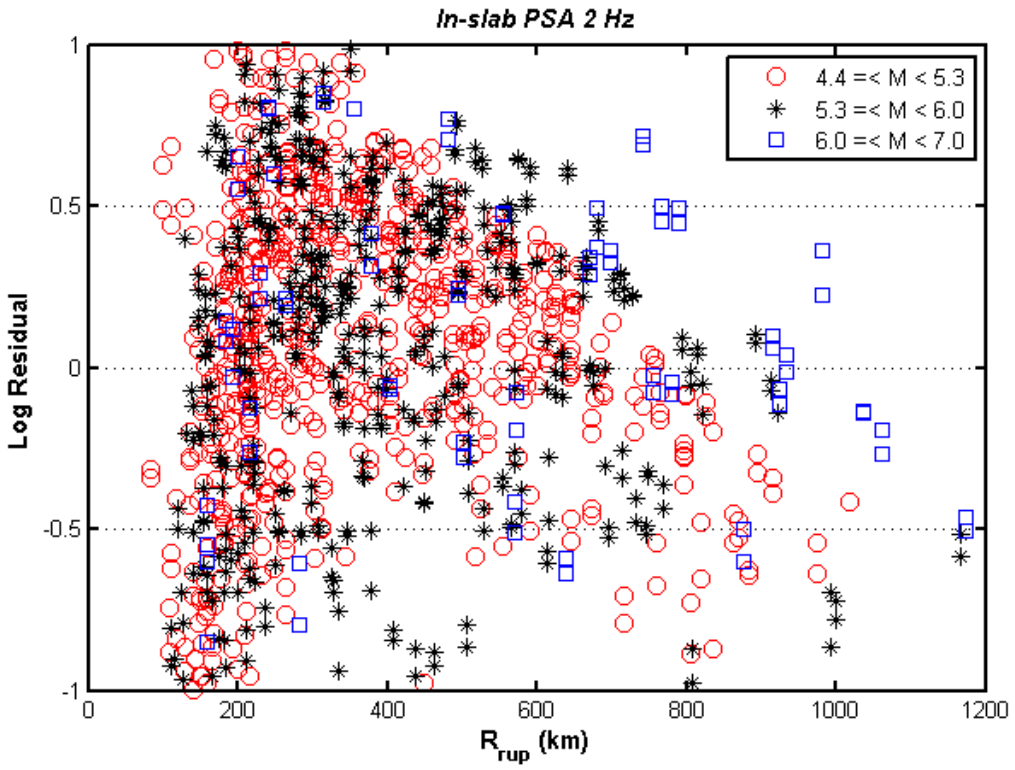

Figure 25 Distribution of log residuals with respect to rupture distance and distinguished by magnitude, for in-slab events at a frequency of 2 Hz.

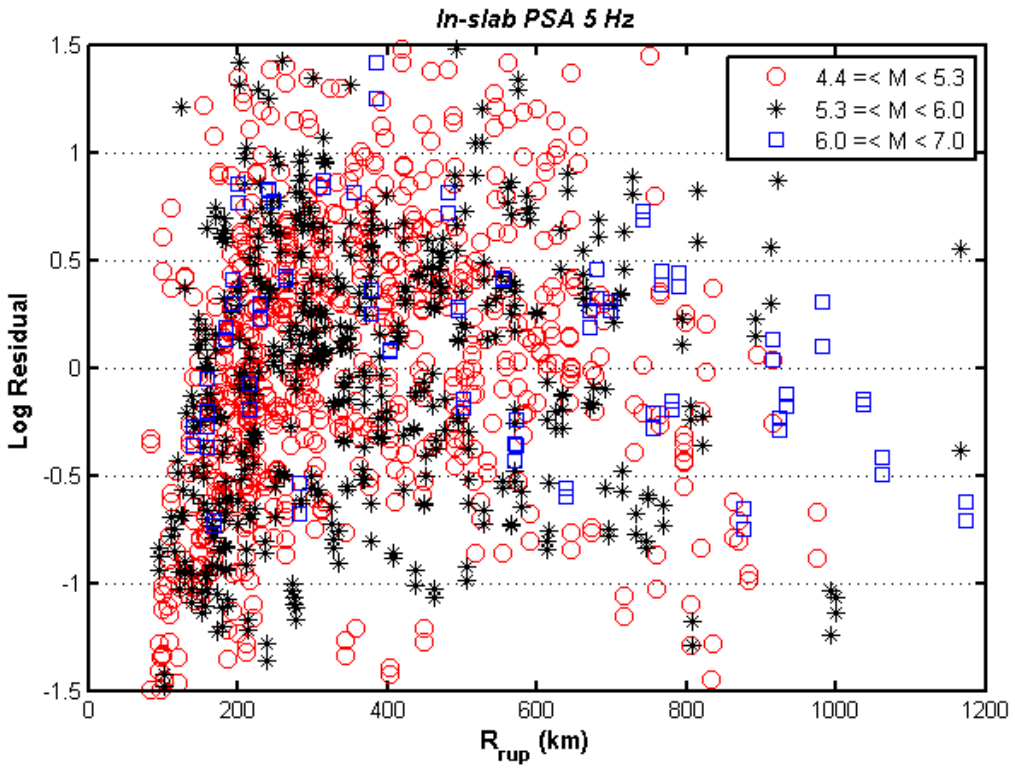

Figure 26 Distribution of log residuals with respect to rupture distance and distinguished by magnitude, for in-slab events at a frequency of 5 Hz.

4.5 Comparisons with Other Studies

For the study region, I am interested in the prediction of ground motions at far-distance events. To evaluate how well the predictive relations are applicable to the region, I analyzed 118 local and regional earthquakes of M 4.0 to 7.0 as listed in Table 1. Since there are no ground-motion predictive relations available for the region, I compare my relations with existing worldwide relations developed for both interface and in-slab events at a range of frequencies. Figures 27 to 50 compare the predictive ground-motion parameters obtained in this study for both interface and in-slab events with existing

predictive relations for subduction earthquakes. In Figures 27 to 50, Youngs-97 and AB-2003 denote Youngs et al. (1997) and Atkinson and Boore (2003) respectively.

Figures 27 to 38 show the interface events, while Figures 39 to 50 plot the in-slab events. Corresponding predictions of Youngs-97 and AB-2003 are also shown. Note that I plot 2.5 Hz of AB-2003 because coefficients for 2 Hz were not available. Figures 27 to 38 indicate that the PGA values predicted for both interface and in-slab events by our relations are significantly lower than those predicted by Youngs-97. On the contrary, PGA values predicted by AB-2003 for all magnitude ranges by our relations are much higher. It is apparent that our relations agree well with the observed data for all predicted values except for the near distance (i.e. distance less than 200 km) events. Note the near-source distances events are of little or no concern for the region as all events that occurred in the region are from far-source distances. A similar pattern is observed for PSA at all frequencies. PSA for both interface and in-slab events predicted by our relations agree reasonably well with the observed data for all magnitudes and frequencies ranges. I note that both Youngs-97 and AB-2003 do not adequately describe the observed ground-motions. This is probably due to the fact that they are based on a much larger global dataset.

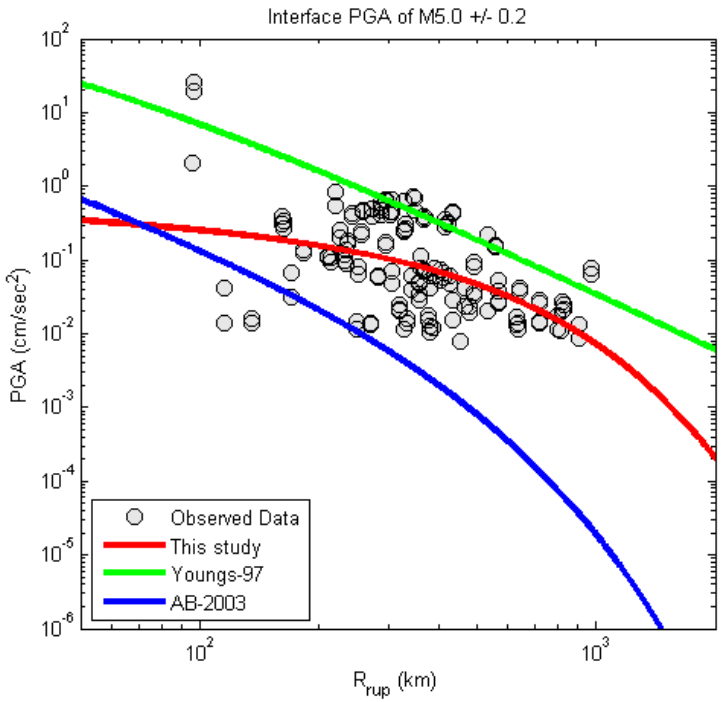

Figure 27 Comparison of ground motion amplitudes predicted by this study for interface earthquakes (H = 20 km) of M 5.0 ± 0.2 at a frequency of 0 Hz (PGA). Corresponding predictions of Youngs et al. (1997) and Atkinson-Boore (2003) are also shown.

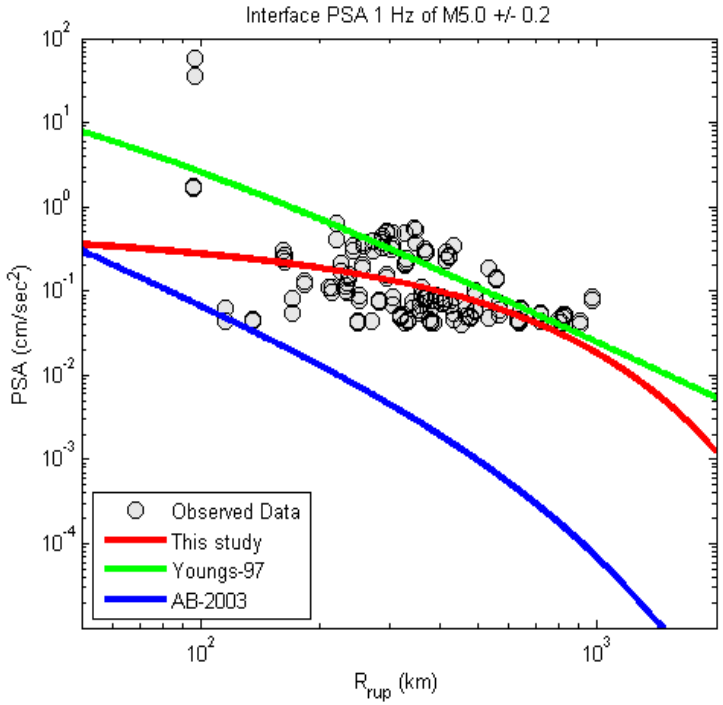

Figure 28 Comparison of ground motion amplitudes predicted by this study for interface earthquakes (H = 20 km) of M 5.0 ± 0.2 at a frequency of 1 Hz. Corresponding predictions of Youngs et al. (1997) and Atkinson-Boore (2003) are also shown.

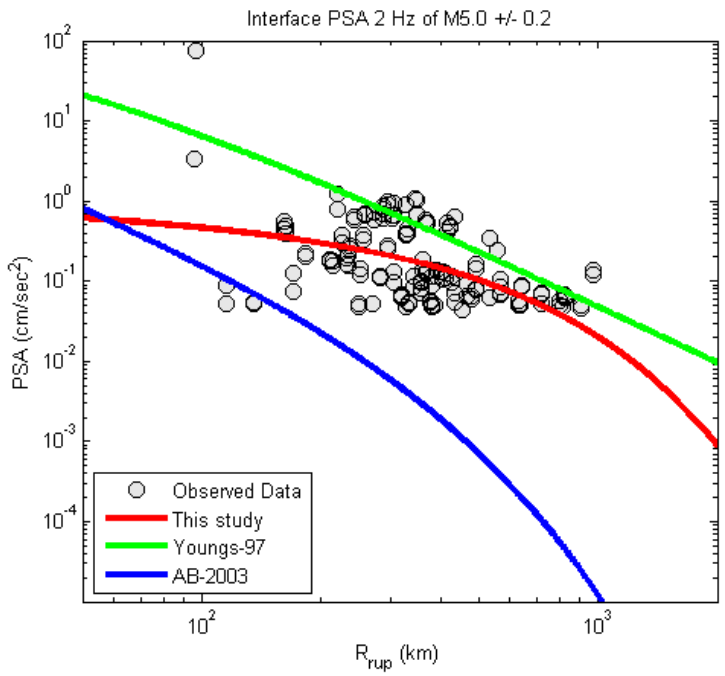

Figure 29 Comparison of ground motion amplitudes predicted by this study for interface earthquakes (H = 20 km) of M 5.0 ± 0.2 at a frequency of 2 Hz. Corresponding predictions of Youngs et al. (1997) and Atkinson-Boore (2003) are also shown.

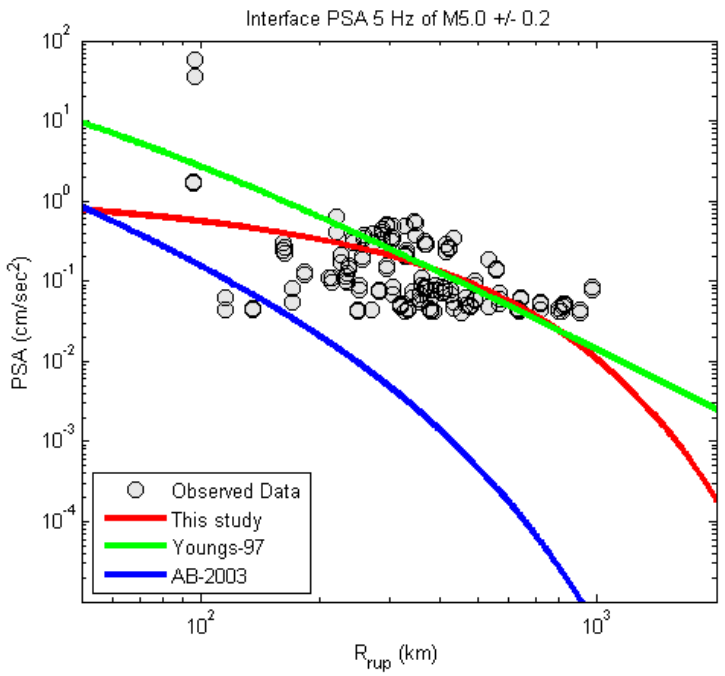

Figure 30 Comparison of ground motion amplitudes predicted by this study for interface earthquakes (H = 20 km) of M 5.0 ± 0.2 at a frequency of 5 Hz. Corresponding predictions of Youngs et al. (1997) and Atkinson-Boore (2003) are also shown.

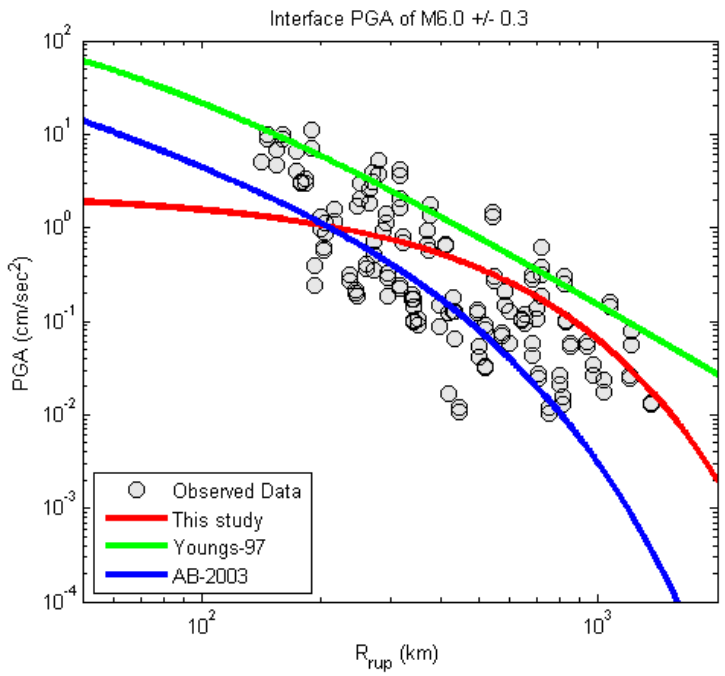

Figure 31 Comparison of ground motion amplitudes predicted by this study for interface earthquakes (H = 38 km) of M 6.0 ± 0.3 at a frequency of 0 Hz (PGA). Corresponding predictions of Youngs et al. (1997) and Atkinson-Boore (2003) are also shown.

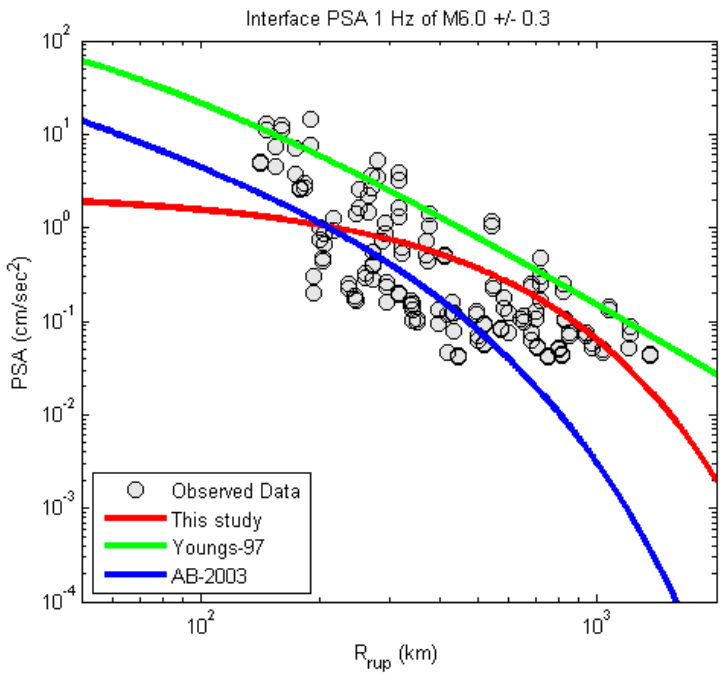

Figure 32 Comparison of ground motion amplitudes predicted by this study for interface earthquakes (H = 38 km) of M 6.0 ± 0.3 at a frequency of 1 Hz. Corresponding predictions of Youngs et al. (1997) and Atkinson-Boore (2003) are also shown.

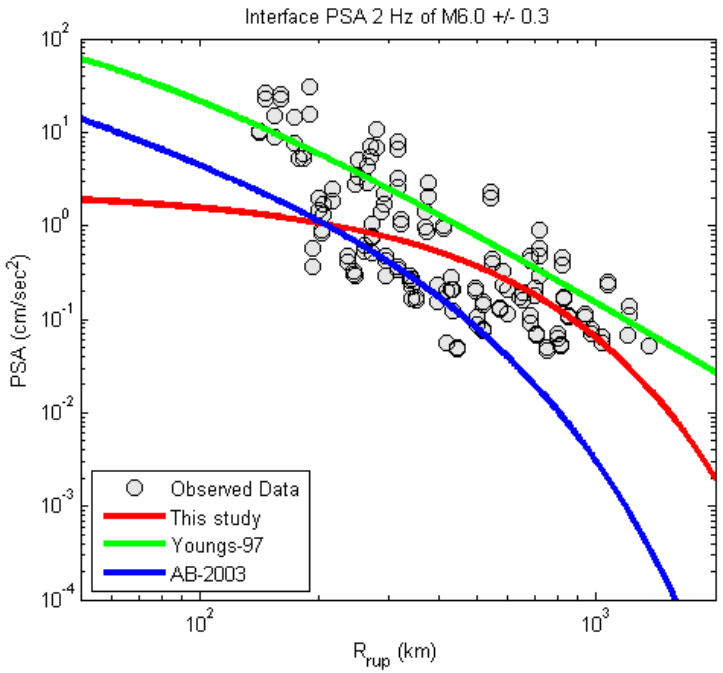

Figure 33 Comparison of ground motion amplitudes predicted by this study for interface earthquakes (H = 38 km) of M 6.0 ± 0.3 at a frequency of 2 Hz. Corresponding predictions of Youngs et al. (1997) and Atkinson-Boore (2003) are also shown.

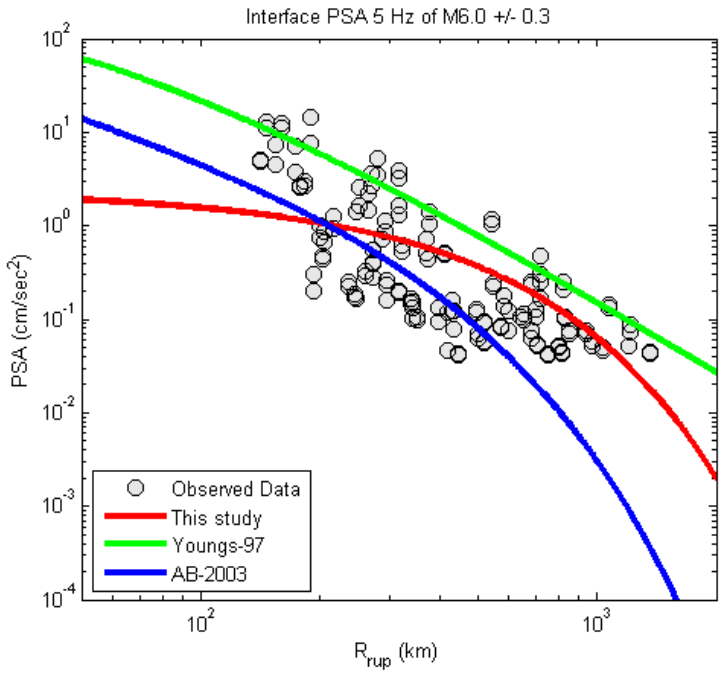

Figure 34 Comparison of ground motion amplitudes predicted by this study for interface earthquakes (H = 38 km) of M 6.0 ± 0.3 at a frequency of 5 Hz. Corresponding predictions of Youngs et al. (1997) and Atkinson-Boore (2003) are also shown.

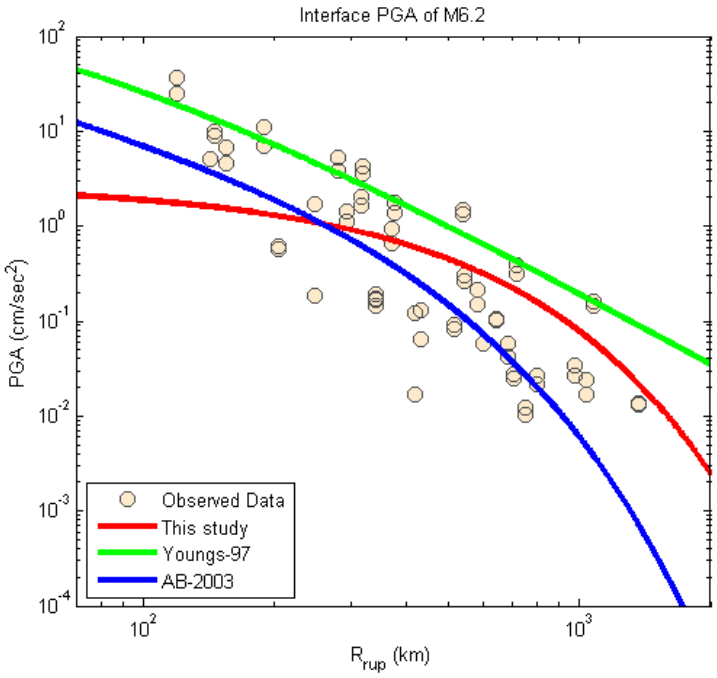

Figure 35 Comparison of ground motion amplitudes predicted by this study for interface earthquakes (H = 35 km) of M 6.2 at a frequency of 0 Hz (PGA). Corresponding predictions of Youngs et al. (1997) and Atkinson-Boore (2003) are also shown.

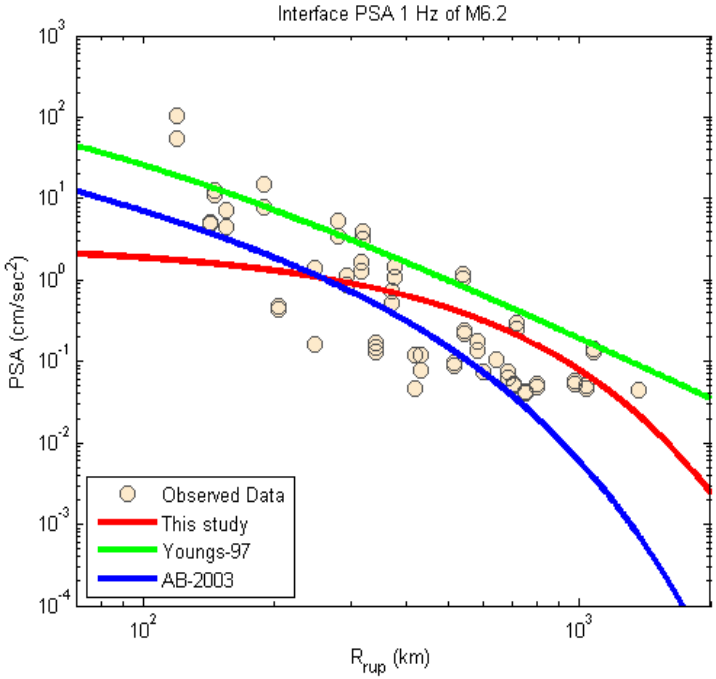

Figure 36 Comparison of ground motion amplitudes predicted by this study for interface earthquakes (H = 35 km) of M 6.2 at a frequency of 1 Hz. Corresponding predictions of Youngs et al. (1997) and Atkinson-Boore (2003) are also shown.

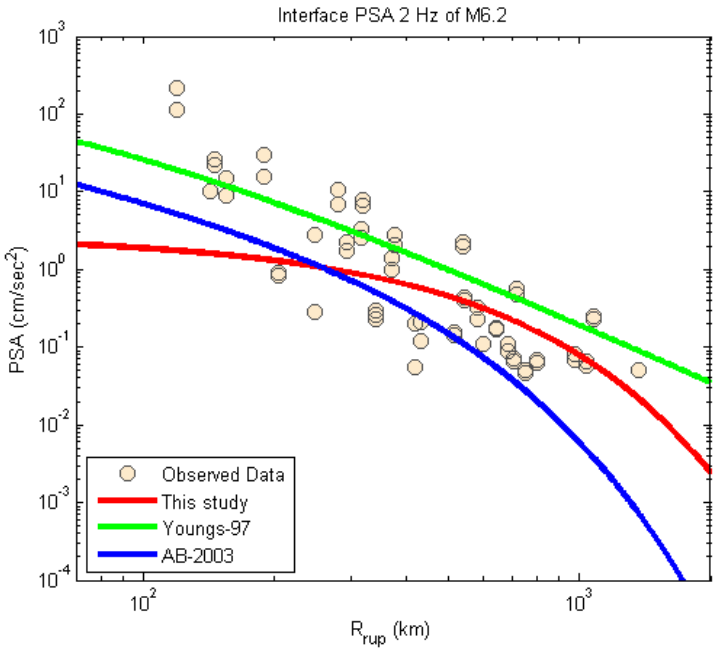

Figure 37 Comparison of ground motion amplitudes predicted by this study for interface earthquakes (H = 35 km) of M 6.2 at a frequency of 2 Hz. Corresponding predictions of Youngs et al. (1997) and Atkinson-Boore (2003) are also shown.

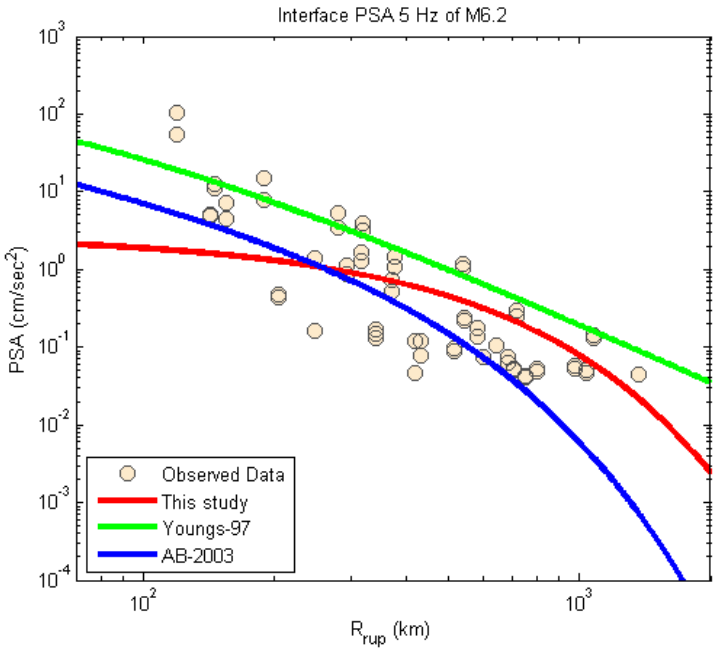

Figure 38 Comparison of ground motion amplitudes predicted by this study for interface earthquakes (H = 35 km) of M 6.2 at a frequency of 5 Hz. Corresponding predictions of Youngs et al. (1997) and Atkinson-Boore (2003) are also shown.

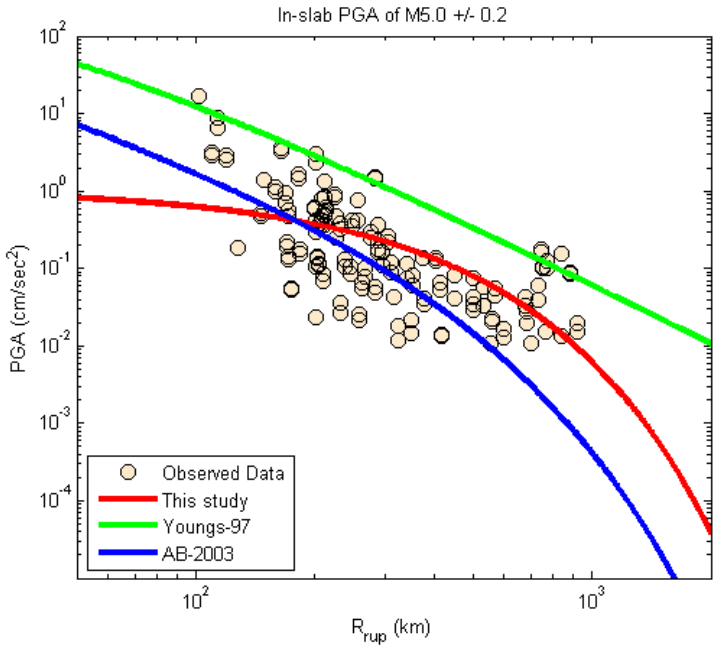

Figure 39 Comparison of ground motion amplitudes predicted by this study for in-slab earthquakes (H = 53 km) of M 5.0 ± 0.2 at a frequency of 0 Hz (PGA). Corresponding predictions of Youngs et al. (1997) and Atkinson-Boore (2003) are also shown.

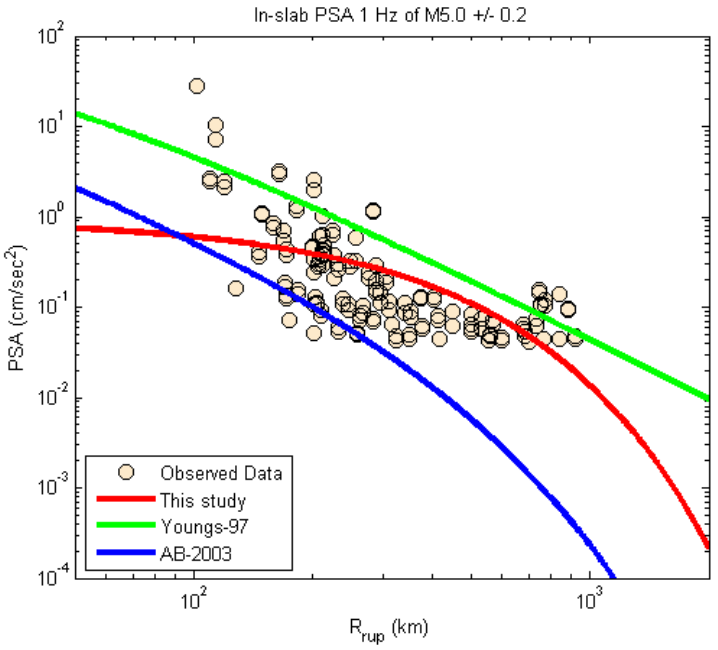

Figure 40 Comparison of ground motion amplitudes predicted by this study for in-slab earthquakes (H = 53 km) of M 5.0 ± 0.2 at a frequency of 1 Hz. Corresponding predictions of Youngs et al. (1997) and Atkinson-Boore (2003) are also shown.

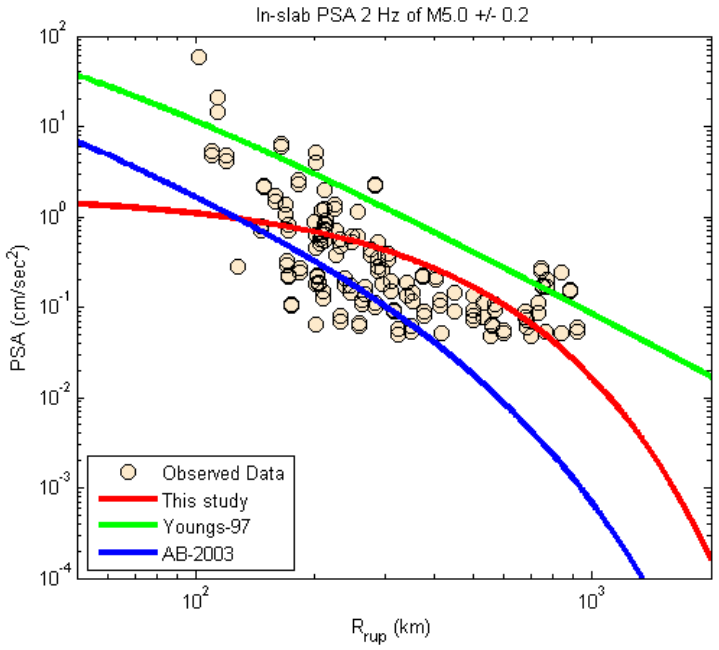

Figure 41 Comparison of ground motion amplitudes predicted by this study for in-slab earthquakes (H = 53 km) of M 5.0 ± 0.2 at a frequency of 2 Hz. Corresponding predictions of Youngs et al. (1997) and Atkinson-Boore (2003) are also shown.

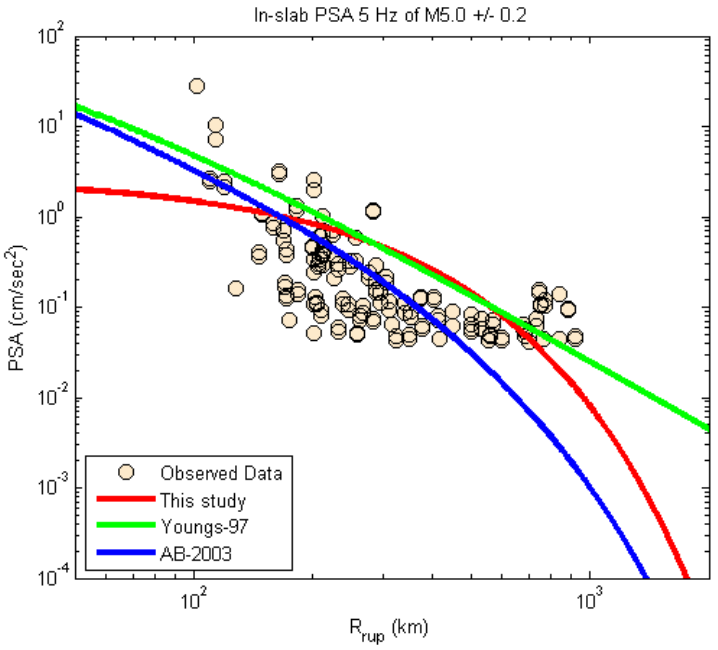

Figure 42 Comparison of ground motion amplitudes predicted by this study for in-slab earthquakes (H = 53 km) of M 5.0 ± 0.2 at a frequency of 5 Hz. Corresponding predictions of Youngs et al. (1997) and Atkinson-Boore (2003) are also shown.

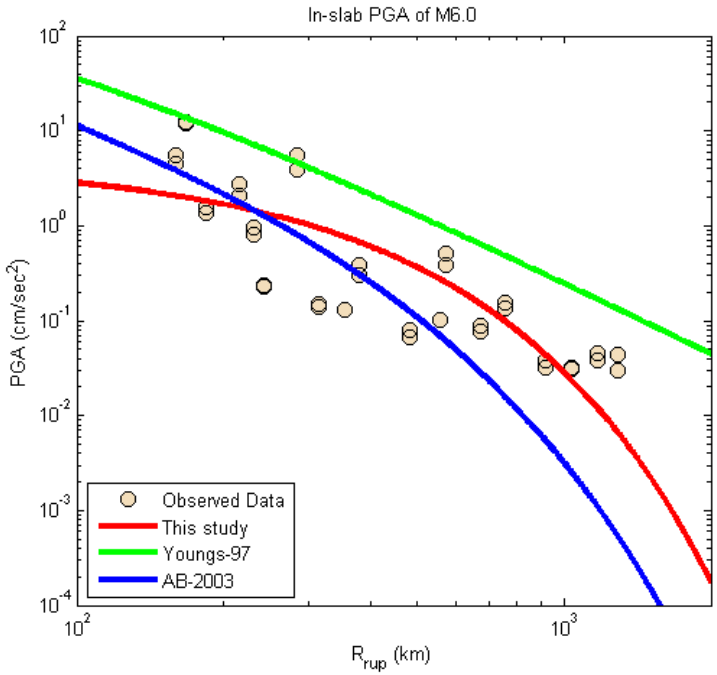

Figure 43 Comparison of ground motion amplitudes predicted by this study for in-slab earthquakes (H = 57.2 km) of M 6.0 at a frequency of 0 Hz (PGA). Corresponding predictions of Youngs et al. (1997) and Atkinson-Boore (2003) are also shown.

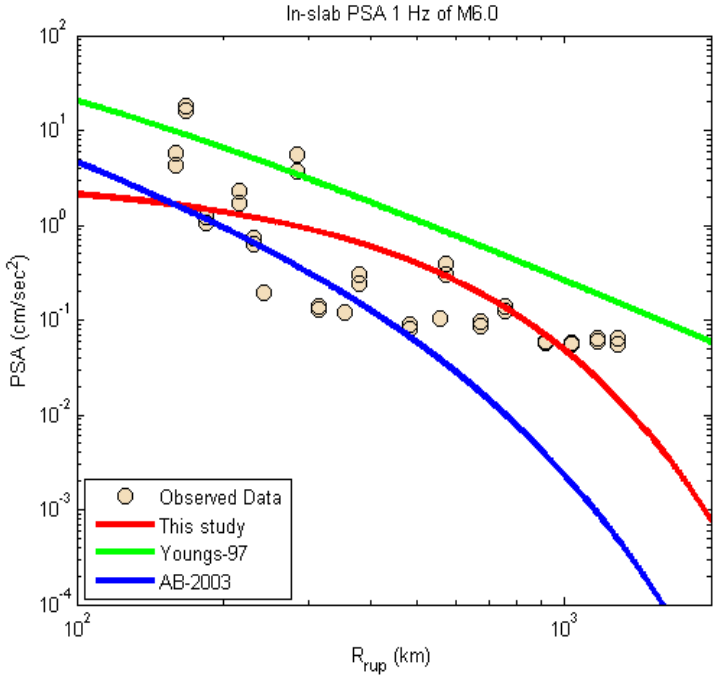

Figure 44 Comparison of ground motion amplitudes predicted by this study for in-slab earthquakes (H = 57.2 km) of M 6.0 at a frequency of 1 Hz. Corresponding predictions of Youngs et al. (1997) and Atkinson-Boore (2003) are also shown.

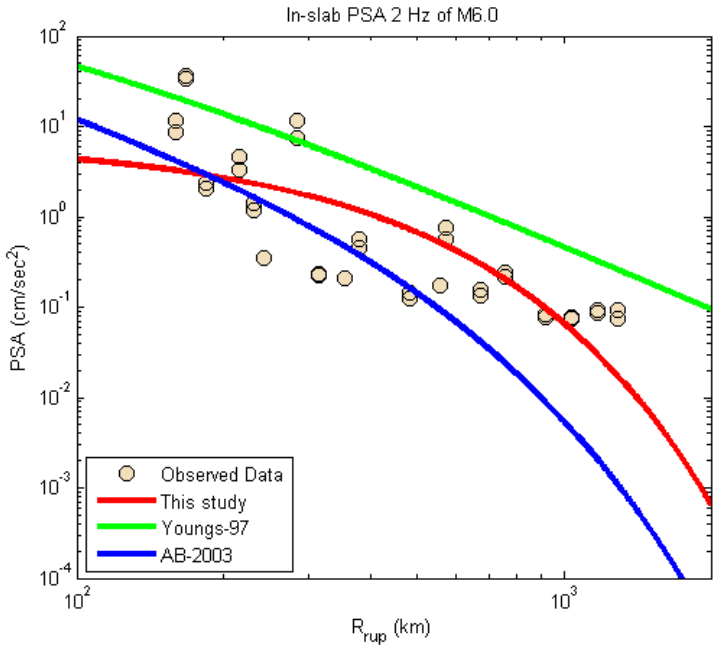

Figure 45 Comparison of ground motion amplitudes predicted by this study for in-slab earthquakes (H = 57.2 km) of M 6.0 at a frequency of 2 Hz. Corresponding predictions of Youngs et al. (1997) and Atkinson-Boore (2003) are also shown.

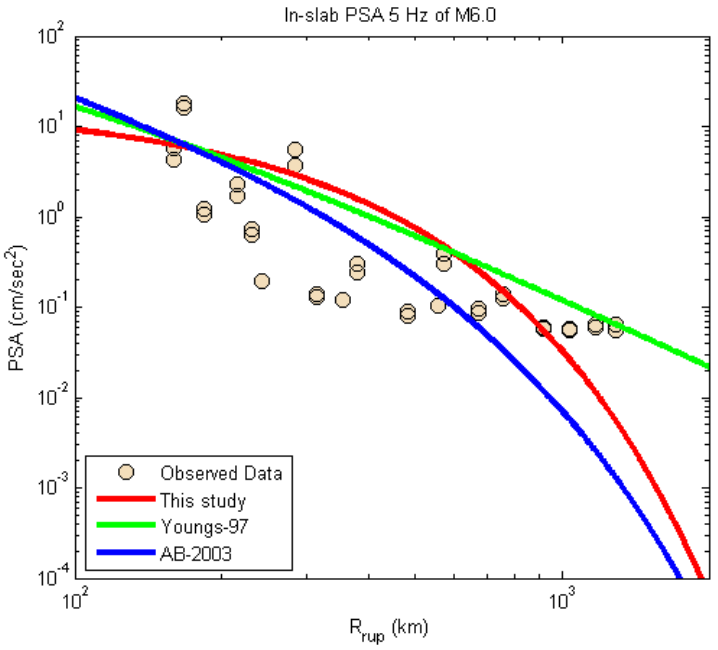

Figure 46 Comparison of ground motion amplitudes predicted by this study for in-slab earthquakes (H = 57.2 km) of M 6.0 at a frequency of 5 Hz. Corresponding predictions of Youngs et al. (1997) and Atkinson-Boore (2003) are also shown.

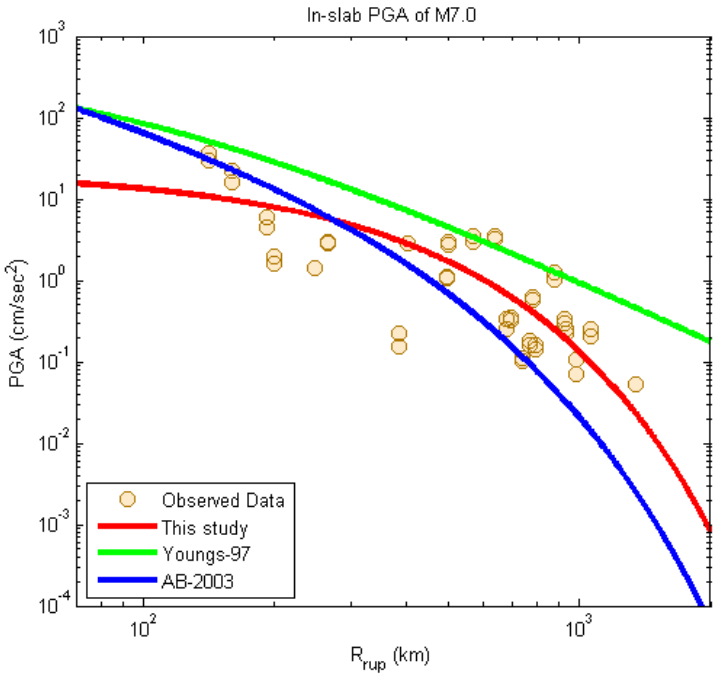

Figure 47 Comparison of ground motion amplitudes predicted by this study for in-slab earthquakes (H = 57.8 km) of M 7.0 at a frequency of 0 Hz (PGA). Corresponding predictions of Youngs et al. (1997) and Atkinson-Boore (2003) are also shown.

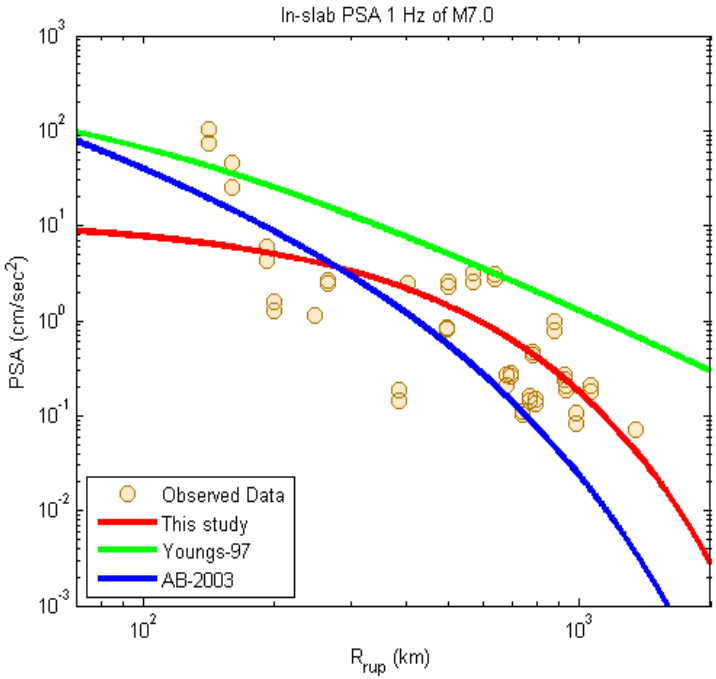

Figure 48 Comparison of ground motion amplitudes predicted by this study for in-slab earthquakes (H = 57.8 km) of M 7.0 at a frequency of 1 Hz. Corresponding predictions of Youngs et al. (1997) and Atkinson-Boore (2003) are also shown.

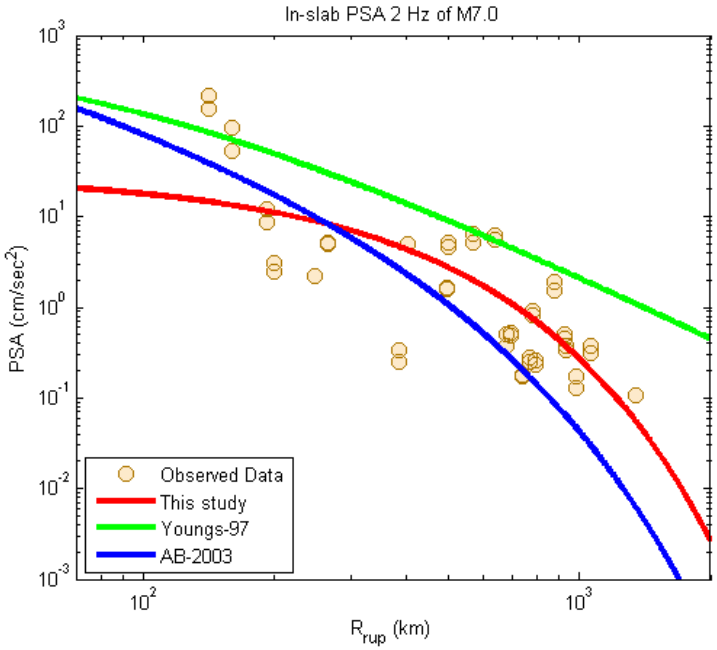

Figure 49 Comparison of ground motion amplitudes predicted by this study for in-slab earthquakes (H = 57.8 km) of M 7.0 at a frequency of 2 Hz. Corresponding predictions of Youngs et al. (1997) and Atkinson-Boore (2003) are also shown.

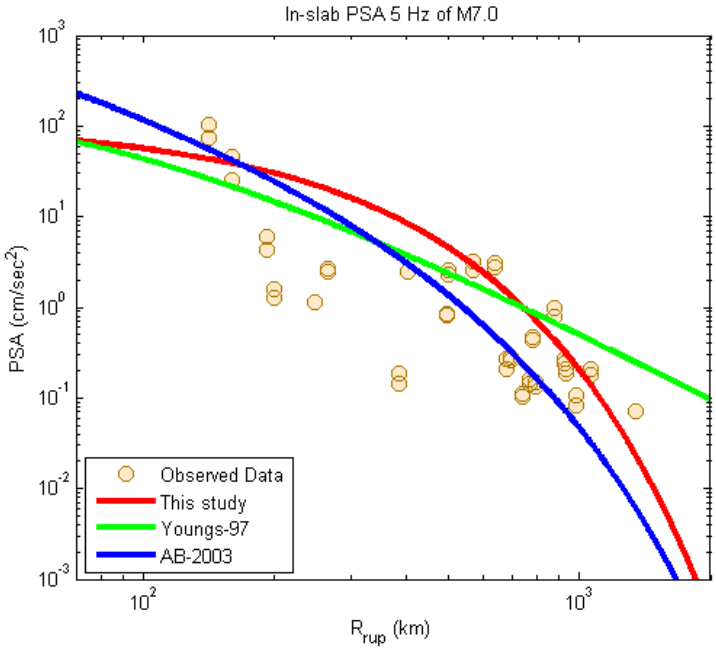

Figure 50 Comparison of ground motion amplitudes predicted by this study for in-slab earthquakes (H = 57.8 km) of M 7.0 at a frequency of 5 Hz. Corresponding predictions of Youngs et al. (1997) and Atkinson-Boore (2003) are also shown.

CHAPTER 5

CONCLUSIONS AND RECOMMENDATIONS

5.1 Conclusions

I have developed empirical ground-motion equations (GMPEs) based on regression of the horizontal-component data compiled from 1,574 digital records of 118 earthquakes of moment magnitude 4.4 to 7.0 that occurred between 2008 and 2013. The relations are appropriate for use for the purpose of estimating ground-motion parameters for PSHA in Java Island. The predictive parameters are PGA and 5% damped PSA at frequencies of 1, 2, and 5 Hz. The developed relations are validated using available recorded data and compared to existing relations for other regions. This is the first empirical region-specific relation for subduction earthquakes for Java Island region. I believe that these equations provide more accurate region-specific relations for the Government of Indonesia to refine and update the building code (SNI 1726-2012) developed in 2010 in order to preserve public safety.

The resultant empirical attenuation relation of the PGA for interface earthquakes is

$$\mathrm{Log}_{10}(Y) = -2.0827 + 0.3826\mathbf{M} + 0.0055H - 0.0015R_{rup} - 10^{(2.6891\ -\ 0.6804\mathbf{M})}\log_{10}(R_{rup})$$

with a standard deviation of 0.6169

and for in-slab earthquakes the relation is

$$\mathrm{Log}_{10}(Y) = -3.1635 + 0.6705\mathbf{M} - 0.0026H - 0.0022R_{rup} - 10^{(-1.5296 - 0.0297\mathbf{M})}\log_{10}(R_{rup})$$

with a standard deviation of 0.6077.

Similar equations are available for response spectra, as shown in Table 4, with σ_{logY} the standard deviation. There are magnitude- and distance-dependent trends in the residuals for these relationships. There is a tendency towards overestimation of the PSA for in-slab events at a frequency of 5 Hz and at large distances (> 300km), but this not critical for engineering applications.

The GMPEs are the most important parameters in probabilistic seismic hazard analysis (PSHA) that used to estimate the hazard level of an earthquake for a specific area. I present GMPEs for interface and in-slab earthquakes occurring in subduction zone located in south of Java Island. These GMPEs are determined by the least square method based on two horizontal components of 1,574 ground motion data from 118 earthquakes of moment magnitude (**M**) greater than or equal to 4.4. The predictions of our GMPEs are generally lower than those of Youngs *et al*. (1997) relations but are higher than those of Atkinson-Boore (2003) relations for all magnitudes and all frequencies.

5.2 Recommendations

This investigation is a preliminary case study for the region. After more ground motion data from Java subduction zone become available, especially from large events, we will need to update and revise this study. We can separate records into rock and soil

classification. Also, it is necessary to use the maximum likelihood method, instead of the least square method, to resolve and mix some problems of data distribution. All the more, it should be possible to develop GMPEs comprehensively for all subduction zones in the Indonesia region.

From this study, I would like to recommend the possibility of improving the following aspects:

- Refining of site amplification factors throughout the region.
- Testing the relation with a richer data set from neighboring countries including a larger number of strong-motion recordings.
- Developing new seismic hazard map for Java Island using these new relations.
- Revising the Indonesian earthquake resistant building code (SNI 1726-2012) with the new specific GMPEs for the Indonesia region.

BIBLIOGRAPHY

Abe, K. (1981). Magnitudes of large shallow earthquakes from 1904 to 1980, *Phys. Earth Planet. Int*. **27**, 72–92.

Abercrombie, R. E., M. Antolik, K. Felzer, and G. Ekstrom (2001). The 1994 Java tsunami earthquake: slip over a subducting seamount, *J. Geophys. Res.* **106,** 6595-6607.

Abrahamson, N. A., and K. M. Shedlock (1997). Overview, *Seism. Res. Lett.* **68,** 9–23.

Allen T. I. and D. J. Wald (2009). Short Note: On the use of high-resolution topographic data as a proxy for seismic site conditions (V_{S30}), *Bull. Seismol. Soc. Am.* **99,** 935–943.

ASCE (2010). Minimum design loads for buildings and other structures, *American Society of Civil Engineers*, No.7, ISBN 978-0-7844-1115-5, Reston, Virginia.

Asrurifak, M., Irsyam, M., Budiono, B., Triyoso, W., and Hendriyawan (2010). Development of spectral hazard map for Indonesia with a return period of 2500 years using probabilistic method, *Civil Engin. Dimens.* **12,** 52-62.

Atkinson, G. M., and D. M. Boore (2003). Empirical ground-motion relations for subduction-zone earthquakes and their application to Cascadia and other regions, *Bull. Seismol. Soc. Am.* **93,** 1703–1729.

Bozorgnia, Y., and Campbell, K. W. (2004). Engineering characterization of ground motion. In *Earthquake Engineering: From Engineering Seismology to Performance-Based Engineering*, Ed. Bozorgnia, Y. and Bertero, V.V., CRC Press, Florida.

Boen, T., S. Wijanto, T. Andriono, and D. H. Natawidjaj (2009). The M7.3 September 2, 2009, West Java quake, EERI Special Earthquake Report, *EERI Newsletter* **43**, October 2009.

Das, R., H. R. Wason, and M. L. Sharma (2011). Global Regression Relations for Conversion of surface Wave and Body Wave Magnitudes to Moement Magnitude, *Nat Hazard* **59,** 801-810.

Douglas, J. (2011). *Ground-motion prediction equations 1964–2010*, Pacific Earthquake Engineering Research Center, University of California, Berkeley, 3-17.

Hall, R. (2002). Cenozoic Geological and Plate Tectonic Evolution of SE Asia and the SW Pacific: Computer Based Reconstruction and Animations, *J. Asian Earth Sci.* **20**, 353-451.

Hutapea, B., B. Rudianto, F. X. Toha, Hartono, A. D. Adi, J. Chavez, E. Hausler, Irwansyah, T. Sriana, and A. Syam (2006). The **M** 6.3 Java, Indonesia, Earthquake of May 27, 2006, EERI Special Earthquake Report, *EERI Newsletter* **40,** August 2006.

Housner, G. W. (1970). *Strong ground motion*, Chapter 4 of *Earthquake Engineering*, Robert L. Wiegel (ed), Pretice-Hall, New Jersey, 75-91.

Irsyam, M., Sengara, I.W., Asrurifak, M., Ridwan, M., Aldiamar, F., Widiyantoro, S., Triyoso, W., Natawijaya, D.H., Kertapati, E., Meilano, I., and Suhardjono (2010). Summary: Development of Seismic Hazard Maps of Indonesia for Revision of Seismic Hazard Map in SNI 03-1726-2002, reseach report submited to the Ministry of Public Works by Team for Revision of Seismic Hazard Maps of Indonesia, July.

IBC (2009). *International Building Code*, International Code Council, Falls Church, Virginia.

Kanamori, H. (1977). The energy release in great earthquakes, *J. Geophys. Res.* **82**, 2981–2987.

Kato, T., T. Ito, H. Z. Abidin, and Agustan (2007). Preliminary report on crustal deformation surveys and tsunami measurements caused by the July 17, 2006 South off Java Island Earthquake and Tsunami, Indonesia, *Earth Planets Space* **59,** 1,055–1,059.

Lin, P., and C. Lee (2008). Ground-Motion Attenuation Relationships for Subduction-Zone Earthquakes in Northeastern Taiwan, *Bull. Seismol. Soc. Am.* **98,** 220-240.

Megawati, K. and T. C. Pan (2010). Ground-motion attenuation relationship for the Sumatran megathrust earthquakes, *Earthquake Enginee. Struct. Dyn.* **39,** 827–845.

Mori, J., Mooney, D. Walter, Afnimar, S. Kurniawan, A. I. Anaya, and S. Widiyantoro (2007). The 17 July 2006 Tsunami Earthquake in West Java, Indonesia, *Seism. Res. Lett.* **78(2),** 201–207.

Okal, E. A. (2012). The south of Java earthquake of 1921 September 11: a negative search for a large interpolate thrust event at the Java Trench, *J. Geophys. Int*. **190**, 1657-1672.

Pacey, A., C. G. Macpherson, K. J. W. McCaffrey (2013). Linear volcanic segments in the central Sunda Arc, Indonesia identified using Hough Transform analysis: Implications for arc lithosphere control upon volcano distribution, *Earth Planet. Sci. Lett.* **369-370,** 24-33.

Scordilis, E. M. (2006). Empirical global relations converting M_S and m_b to moment magnitude, *J. Seism.* **10,** 225–236.

Simons, W.J.F., A. Socquet, C. Vigny, B. A. C. Ambrosius, S. H. Abu, C. Promthong, C. Subarya, D. A. Sarsito, S. Matheussen, P. Morgan, W. Spakman (2007). A decade of GPS in Southeast Asia: resolving Sundaland motion and boundaries, *J. Geophys. Res.* **112**, 1-20.

SNI-1726 (2012). *Indonesian Earthquake Resistant Building Code*, National Standardization Agency of Indonesia (BSN), Jakarta (in Indonesian).

Suhardjono (2010). Jarinagan Accelerograph BMKG, *Presented in Workshop Peningkatan Jaringan Monitoring Gempabumi Kuat*, Jakarta, 15 October 2010.

Tsuji, T., K. Yamamoto, T. Matsuoka, Y. Yamada, K. Onishi, A. Bahar, I. Meilano, and H. Z. Abidin (2009). Earthquake fault of the 26 May 2006 Yogyakarta earthquake observed by SAR inferometry, *Earth Planets Space* **61,** e29-e32.

Tichelaar, B. W., and L. J. Ruff (1993). Depth of seismic coupling along subduction zones, *J. Geophys. Res.* **98**, 2017–2037.

Tsuji, Y., F. Imamura, H. Matsutomi, C. E. Synolakis, P. T. Nanang, Jumadi, S. Harada, S. S. Han, K. Arai, and B. Cook (1995). Field survey of the East Java earthquake and tsunami of June 3, 1994, *PAGEOPH* **144**, 3-4.

The Consultative Group on Indonesia (CGI) (2006). Preliminary damage and loss assessment, *Yogyakarta and Central Java Natural Disaster*: A Joint Report from BAPPENAS, the Provincial and Local Governments of D.I. Yogyakarta, the Provincial and Local Governments of Central Java, and International Partners, Jakarta.

Wald, D. J. and T. I. Allen (2007). Review Article: Topographic slope as a proxy for seismic site conditions and amplification, *Bull. Seismol. Soc. Am.* **97,** 1379–1395.

Wells, D.L. and K. J. Coppersmith (1994). New empirical relationships among magnitude, rupture length, rupture width, rupture area, and surface displacement, *Bull. Seismol. Soc. Am.* **84,** 974–1002.

Youngs, R. R., S. J. Chiou, W. J. Silva, and J. R. Humphrey (1997). Strong ground motion attenuation relationships for subduction zone earthquakes, *Seism. Res. Lett.* **68(1)**, 58–73.

Zhao, J. X., J. Zhang, A. Asano, Y. Ohno, T. Oouchi, T. Takahashi, H. Ogawa, K. Irikura, H. K. Thio, P. G. Somerville, and Y. Fukushima (2006). Attenuation relations of

strong ground motion in Japan using site classification based on predominant period, *Bull. Seismol. Soc. Am.* **96(3),** 898–913.

Vitae

Name	: Abdul Latif
Nationality	: Indonesia
Date of Birth	: August 06, 1989
Email	: latif.demak@gmail.com
Address	: Bener Rt: 005/002 Weding, Bonang, Demak, Central Java, Indonesia 59552.
Academic Background	: B.Sc. in Physics (Geophysics concentration) from Diponegoro University, Semarang, Indonesia in 2011.
List Of Publications	: Probabilistic Seismic Hazard Analysis for Central Java Province, Indonesia (2015), accepted in Bulletin of Seismological Society of America (BSSA).
	Analysis of Microseismic Events during a Multi-stage Hydraulic Stimulation Experiment at a Shale Gas Reservoir, accepted in 2015 Joint Assembly: American Geophysical Union (AGU) - Canadian Geophysical Union (CGU), Canada.
	Ground-Motion Relations for Subduction-Zone Earthquakes in Java Island, Indonesia (2015), submitted in Journal of Seismology.
	Analyzing Earthquake Patterns and Calculating the Gutenberg-Richter Parameters: Java Island, Indonesia, as a Case Study (2014), accepted in 5th Student Scientific Conference at KFUPM.